

5-1-2019

High-Pressure High-Temperature Exploration of Phase Boundaries Using Raman Spectroscopy

Jasmine Kashmir Hinton
jasminebishop715@yahoo.com

Follow this and additional works at: <https://digitalscholarship.unlv.edu/thesesdissertations>



Part of the [Condensed Matter Physics Commons](#), [Optics Commons](#), and the [Other Physics Commons](#)

Repository Citation

Hinton, Jasmine Kashmir, "High-Pressure High-Temperature Exploration of Phase Boundaries Using Raman Spectroscopy" (2019). *UNLV Theses, Dissertations, Professional Papers, and Capstones*. 3613. <https://digitalscholarship.unlv.edu/thesesdissertations/3613>

This Thesis is protected by copyright and/or related rights. It has been brought to you by Digital Scholarship@UNLV with permission from the rights-holder(s). You are free to use this Thesis in any way that is permitted by the copyright and related rights legislation that applies to your use. For other uses you need to obtain permission from the rights-holder(s) directly, unless additional rights are indicated by a Creative Commons license in the record and/or on the work itself.

This Thesis has been accepted for inclusion in UNLV Theses, Dissertations, Professional Papers, and Capstones by an authorized administrator of Digital Scholarship@UNLV. For more information, please contact digitalscholarship@unlv.edu.

HIGH-PRESSURE HIGH-TEMPERATURE EXPLORATION OF PHASE BOUNDARIES USING
RAMAN SPECTROSCOPY

By

Jasmine K. Hinton

Bachelor of Science—Physics
University of Utah
2016

A thesis submitted in partial fulfillment
of the requirements for the

Master of Science—Physics

Department of Physics and Astronomy
College of Sciences
The Graduate College

University of Nevada, Las Vegas
May 2019

Copyright [2019] by [Jasmine Hinton]

All Rights Reserved



Thesis Approval

The Graduate College
The University of Nevada, Las Vegas

April 11, 2019

This thesis prepared by

Jasmine K. Hinton

entitled

High-Pressure High-Temperature Exploration of Phase Boundaries Using Raman Spectroscopy

is approved in partial fulfillment of the requirements for the degree of

Master of Science - Physics
Department of Physics and Astronomy

Ashkan Salamat, Ph.D.
Examination Committee Chair

Kathryn Hausbeck Korgan, Ph.D.
Graduate College Dean

Qiang Zhu, Ph.D.
Examination Committee Member

Liping Wang, Ph.D.
Examination Committee Member

Jason Steffen, Ph.D.
Examination Committee Member

Pamela Burnley, Ph.D.
Graduate College Faculty Representative

Abstract

Metastability of states can provide interesting properties that may not be readily accessible in a material's ground state. Many materials show high levels of polymorphism, indicating a rich energy landscape and a potential for metastable states. Melt crystallization techniques provide a potential route to these states. We use a resistively heated diamond anvil cell (DAC) with fine control of a system's pressure and temperature to explore these systems. Raman spectroscopy is used to track subtle structural changes across phase boundaries. Organic systems, such as glycine and aspirin, were our initial interest due to their high polymorphism and reported low melting temperatures; however, complications with these systems ultimately showed that they are not ideal candidates for this technique. Metallic systems with allowed Raman modes are better samples for this method. We successfully map the phase stability of β -tin under high pressure and temperature conditions using Raman spectroscopy.

Acknowledgements

Committee members for their guidance and participation in this project: Dr. Ashkan Salamat, Dr. Qiang Zhu, Dr. Jason Steffen, and Dr. Pamela Burnley.

The entire Salamat lab family for their work in building a stellar lab in which great measurements can be made, in particular, Dr. Dean Smith, Christian Childs, and Dr. Ashkan Salamat for their work in creating a Raman system capable of making such excellent measurements.

Dr. Elissaios Stavrou at Lawrence Livermore National Lab for the terrific mentoring during time spent there.

Paul Ellison and Bill O'Donnell for their contributions in the development of the resistive heating rig for the diamond anvil cell.

Dedication

I dedicate this work to my husband, Joel, and to my fur daughters, Marcie and Piper, for their love and moral support throughout this process.

Table of Contents

| | |
|--|------|
| Abstract | iii |
| Acknowledgements | iv |
| Dedication | v |
| Table of Contents | vi |
| List of Tables | vii |
| List of Figures | viii |
| Introduction | 1 |
| Energy Landscapes and Metastable States | 1 |
| Pressure and temperature: windows for observing nature's phenomenon | 1 |
| Motivation and Sample selection | 2 |
| Background and Motivation of Instrumentation | 3 |
| Methods | 4 |
| Diamond Anvil Cells/High Pressure History | 4 |
| Pressure Markers | 6 |
| Resistive Heating Development | 8 |
| Raman Spectroscopy | 12 |
| Case Studies | 15 |
| The Resistive Heating Story: | 16 |
| <i>Glycine Results</i> | 16 |
| <i>Aspirin Results</i> | 21 |
| <i>Simple Organics Discussion</i> | 26 |
| <i>β-Sn Results</i> | 28 |
| <i>β-Sn Discussion</i> | 33 |
| Related Work: | 36 |
| <i>α-glycine EOS and Raman</i> | 36 |
| <i>Resistive heating at HPCAT</i> | 36 |
| Conclusions | 37 |
| References | 38 |
| Curriculum Vitae | 43 |

List of Tables

| | |
|--|---|
| Table 1: A literature review of pressure markers..... | 7 |
| Table 2: Literature review of resistive heating experiments..... | 9 |

List of Figures

| | |
|---|----|
| Figure 1: Diamond Anvil cell. A) Annotated cross section schematic of Diamond Anvil Cell (DAC) and B) sample chamber loaded with tin, NaCl, and Ruby sphere in stainless steel gasket | 4 |
| Figure 2: Diamond Anvil Cells (DACs) Paul Ellison- Ashkan Salamat (PEAS) Design..... | 5 |
| Figure 3: Stages of creation for the resistive heaters..... | 10 |
| Figure 4: Diamond anvil cell with ceramic backing plates used in a resistive heating experiment.... | 11 |
| Figure 5: Annotated cross sectional diagram of the resistive heating diamond anvil cell setup | 12 |
| Figure 6: Comparison of glycine polymorph morphologies. A) α -glycine and B) β -glycine | 16 |
| Figure 7: Raman stack plot of glycine as a function of temperature..... | 17 |
| Figure 8: Glycine turning opaque as temperature increases (A to D). Transmission lighting geometry used. | 18 |
| Figure 9: Glycine heated at ambient pressures on glass slide (no cover slide) to 230C..... | 19 |
| Figure 10: Raman stack plot of glycine as a function of temperature. After disappearing well before the reported temperatures, the Raman modes never fully returned. | 20 |
| Figure 11: Melt product of aspirin. A) Melt product observed in our lab. B) Spherulite melt product of aspirin-IV measured by Shtukenberg et al | 21 |
| Figure 12: Raman stack plot of a small selection of aspirin modes. Between \sim 200-220C, a negative shift in frequency is observed. This is due to a loss of pressure (known because of Sm:YAG pressure Data) rather than due to temperature..... | 22 |
| Figure 13: Raman stack plot of a set of crystals grown from slow evaporation. Only selection of the modes of aspirin phase I are shown here. Modes labeled in red did not appear in literature..... | 23 |
| Figure 14: Mapping of where Raman spectra were taken for aspirin in phase space. Points with the same shape indicate the same temperature cycle. Points found in the red region were identified as phase I while points in the grey region were identified as phase III. | 25 |

Figure 15: Single crystal of aspirin phase I in an Ar PTM with Sm: YAG crystal loaded in DAC. A) and C) are transmission lighting geometry while B and D are reflected lighting geometry. A) and B) are before heating while C) and D) are after heating. The sample becomes opaque when heated.26

Figure 16: Tin in diamond anvil cell showing visual evidence of melting as a function of temperature and time.....30

Figure 17: SrB₄O₇:Sm²⁺ fluorescence spectra stack plot as a function of temperature.31

Figure 18: Raman spectroscopy stack plot of tin as a function of temperature across melt boundary.32

Figure 19: Raman spectroscopy stack plot of tin as a function of temperature across a solid-solid phase boundary.....33

Figure 20: Phase diagram mapping the phase stability of β -Sn.....34

Figure 21: Raman stack plot of CaCO₃ as a function of temperature. The ratios of the Stokes to Anti-Stokes intensities of a mode can be used to calculate absolute temperature.35

Introduction

Energy Landscapes and Metastable States

Matter exists in many phases and structures. A material's energy landscape is a mapping of all the possible structures a material may take under differing thermodynamic conditions and energies. The lowest energy state is the ground state, and other stable, but higher energy states are considered metastable. For example, one of carbon's metastable states is diamond, while its ground state is graphite at ambient conditions; diamond and graphite have wildly different properties heavily exploited for very different uses. Understanding a material's complete energy landscape often requires complex computation; pressure and temperature are needed to experimentally sample the energy landscapes of materials and provide some insight into the structural complexities of a material.

Pressure and temperature: windows for observing nature's phenomenon

High pressure and temperature are frequently applied to understand materials and their interesting properties. The use of high pressure alone can induce magnetic or superconducting properties, help us understand planetary sciences more deeply, and facilitate synthesis of new materials [1]. High temperature is a valuable technique for relieving the anisotropic strain that can arise from the uniaxial compression of diamond anvil cells [2]. High pressure and temperature can be used to investigate a material's melt curve [3]. The use of high temperature can be used to discover new phases from the melt [4], a property that could potentially be described by a property called Ostwald's rule. Ostwald's rule of stages is an empirical observation by Wilhelm Ostwald made in 1897 stating that the most stable polymorph will not crystallize out of a melt or solution first, but rather the least stable polymorph [5], [6]. This concept inspired us to explore simple organic systems in search of new polymorphic forms under high pressure and temperature conditions.

Motivation and Sample selection

Simple organic systems have rich energy landscapes, providing for the possibility of a large number of unique or metastable states. Many practical reasons to explore polymorphism of simple organics under high pressure and temperatures exist besides interest in them from a basic research perspective[7]. For example, molecular shape is important for how pharmaceutical drugs interact with biological systems. Thus, knowing how a material behaves under a range of conditions, particularly how its structure changes, is helpful for pharmaceutical developers so that they can create a drug with improved functionality. Our technique is particularly relevant to delicate energetic materials systems. Studying energetic materials under pressure or temperature can be challenging even under the best circumstances and often requires strict rules on handling. Using a surrogate organic system with specific similarities to the energetic material potentially provides insight as to how the energetic system might behave in a safe way and allows for the possibility of future large volume press work.

Understanding the structures of organic systems under high pressure and temperature conditions is most certainly important, which makes the difficulty of solving such structures a paramount problem to address. Organic systems often have incredibly complex structure solutions due to the large unit cell made up of molecules rather than single atoms like many physicists may be accustomed to. In order to address this, we are partnered with a talented theoretical group who routinely uses first principles structure solving programs like USPEX to help us solve for the ground state structure[4], [8], [9].

Although simple organic systems began as our initial motivation, they proved to be too complex for a system under development. The Case Studies chapter details our progress with these systems including our challenges, and describes how we moved to address our more fundamental questions about the instrumentation and methods development with more robust systems.

Background and Motivation of Instrumentation

Reaching the correct temperature conditions for a variety of systems merited the application of a tool with precise control, accurate temperature measurement, and the ability to reach and maintain a particular temperature range. Although CO₂ laser heating systems are well equipped to deal with wide bandgap insulators, the risk of decomposition of simple organics is high. Melting temperatures of organic samples considered in this study are relatively low (see section Case studies (glycine and aspirin)), and reaching those temperatures slowly from ambient conditions in order to achieve a steady state is of paramount importance. When considering other systems, specifically tin, both traditional laser heating and resistive heating have been used [10], thus some literature is available to compare to. Measuring the temperature of the sample during heating is arguably one of the most important tasks of any heating experiment. Ohmic heating has the advantage of being able to use thermocouples, which although convenient, give rise to systematic errors. A particularly powerful method of temperature determination of the sample is the use of Raman spectroscopy as an absolute measurement of temperature.

Our goal for the first phase of ohmic heating was to attain fine heating control and measurement of temperature, and to define a set of criteria for sample evolution under high pressure and temperature conditions. This characterization will lend strength to our next generation of resistive heating. The Methods section describes the current progress in our field in ohmic heating, the development of our first phase of ohmic heating, and our robust measurement of temperature used to characterize ohmic heating experiments.

Methods

This chapter gives a brief background on the topics required to understand our research and also describes how we use these techniques to perform our experiments.

Diamond Anvil Cells/High Pressure History

High pressure has been in use as a tool to study material science since the early 20th century. A variety of high pressure devices were employed early on [11], and many important results were gleaned from these early studies [12], [13]. An invention in the 50's and 60's revolutionized high pressure work; the creation of the diamond anvil cell (DAC) gave scientists a literal window into nature previously unobserved [11], [14], [15]. The diamond anvil cell exploits the unique properties of diamond, such as its hardness and optical transparency, to generate ultra-high pressures while allowing direct observation with a variety of techniques during the measurement. Just last year, in 2018, the diamond anvil cell celebrated its 60th anniversary —the diamond anniversary[15].

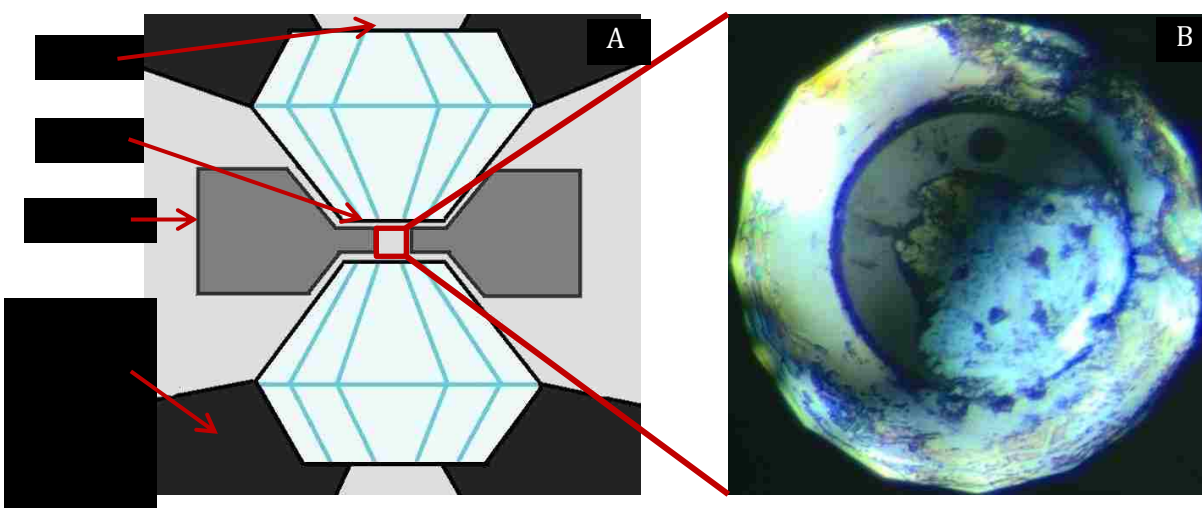


Figure 1: Diamond Anvil cell. A) Annotated cross section schematic of Diamond Anvil Cell (DAC) and B) sample chamber loaded with tin, NaCl, and Ruby sphere in stainless steel gasket

Diamond anvil cells apply uniaxial compression to a sample between two diamonds with flattened tips called culets. Early experiments used only the diamonds to compress the sample with no containment[15], but most modern experiments employ a gasket—a thin sheet of metal indented with the diamond footprint and drilled to have a sample chamber[16]. Setting the dimensions of the gasket, such as the indentation thickness and the diameter of the sample chamber, depends on the needs of the experiment. Anecdotally, we will note that gasket dimensions are a topic of some consideration and debate in the high pressure field. In addition to careful consideration of the gasket conditions and material, the selection of the pressure transmitting medium (PTM) matters for how much of a deviation in pressure a sample will experience across the diamond culet [17]. A liquid PTM, such as liquid He, provides a uniform pressure transmission to the sample up to a certain pressure beyond which we consider it to be quasi-hydrostatic. Careful selection of the correct PTM for the experiment can greatly reduce non-uniform pressure application and the pressure gradient experienced.



Figure 2: Diamond Anvil Cells (DACs) Paul Ellison- Ashkan Salamat (PEAS) Design

Our diamond anvil cells are designed by Ashkan Salamat and Paul Ellison, and machined by Paul Ellison. They are a piston-cylinder type DAC that are optimized for reaching megabar conditions. Our experiments used brilliant and conical cut diamonds with 300 μm , 400 μm , or 600 μm culets depending on our needs and availability of diamonds in stock. Stainless steel gaskets were sufficient for our experimental needs, particularly since reaching ultra-high pressures and having a pure elemental gasket for x-ray diffraction were not our goals for the time being. We specify the thickness after indentation and sample chamber diameter for each experiment as it is relevant. Tungsten carbide backing plates to seat the diamonds were used for most of our experiments, but for our later work, we developed ceramic backing plates to promote thermal isolation of the sample from our heaters (see Methods; Resistive heating and Case Studies; $\beta\text{-Sn}$).

Pressure Markers

Measuring pressure inside the sample chamber of a diamond anvil cell is a critical component of high pressure experiments. A large body of work exists to define a calibrated pressure scale using various techniques and pressure markers. In this manuscript, we include a table reviewing a few popular fluorescence markers from literature. We note that other pressure markers exist for the techniques of x-ray diffraction (such as gold), and Raman Spectroscopy (such as diamond), but we do not discuss them much here, since they are less pertinent to the specific project contained within this work.

Table 1: A literature review of pressure markers.

| Authors | Year | Pressure marker | Maximum Calibration Pressure | Maximum Calibration Temperature | Pressure transmitting medium | Calibration techniques (or additional notes) |
|-----------------------|------|--|------------------------------|---------------------------------|---------------------------------|---|
| Rashchenko et al [18] | 2015 | SrB ₄ O ₇ :Sm ²⁺ | 60 GPa | ambient | He | Sm:YAG used as reference |
| Jing et al [19] | 2013 | SrB ₄ O ₇ :Sm ²⁺ | 48 GPa, 128 GPa | ambient | Ar, no PTM | Gold EOS, yield strength measured |
| Datchi et al [20] | 1997 | SrB ₄ O ₇ :Sm ²⁺ | 124 GPa, 130 GPa | 900K | He, H ₂ O | Ruby chip fluorescence, gold powder EOS |
| Trots et al [21] | 2013 | Sm: YAG | 58 GPa | ambient | Ne or He | Direct measurement of EOS of Sm: YAG |
| Raju et al [22] | 2011 | Ruby Sm: YAG SrB ₄ O ₇ :Sm ²⁺ | 25 GPa | ~ 800K | Ar | EOS of each pressure marker compared to NaCl or Au EOS |
| Goncharov et al [23] | 2005 | Ruby Sm: YAG SrB ₄ O ₇ :Sm ²⁺ | 95 GPa | 850K | H ₂ , N ₂ | Comparison to existing calibrations of Au EOS plus c-BN Raman |
| Dewaele et al [24] | 2008 | Ruby | 65 GPa (Co), 200 GPa (Fe) | Ambient | He | Fe, Co, Ni, Zn, Mo, Ag EOS with XRD related to RSW-EOS |
| Mao et al [25] | 1986 | Ruby | 100 GPa | Ambient | | Ag, Mo, Ag, Pd EOS with XRD related to RSW-EOS |
| Liu et al [26] | 2013 | Ruby | N/A | N/A | N/A | A summary of many Ruby calibrations, and a theoretical correction suggested based on error analysis |

Ruby fluorescence is a common pressure marker, mainly for its ease of acquirement and measurement. Known problems exist with using ruby as a pressure marker at high temperature, including the R1-R2 doublet broadening, the signal-to-background ratio decreasing, and that the R1 temperature dependence is high resulting in a large error in pressure from a small uncertainty in temperature[27]. These factors make resolving the fluorescence spectra difficult and lead to high uncertainties when calculating the pressure at high temperatures. Calibrations exist that account for ruby's behavior under these conditions[27], but better pressure markers are readily available, including those that use fluorescence for scientists looking to keep the same technique. Two of

those are Sm: YAG, and SrB₄O₇:Sm²⁺. We have used both pressure markers in our experiments. We used the calibration for Sm: YAG given in the work Trots et al [21] and for SrB₄O₇:Sm²⁺ we used the reference found in Rashchenko et al [18], and other works that contribute to this characterizing this pressure marker can be found in our summary table. SrB₄O₇:Sm²⁺ in particular is not temperature dependent, maintains a fair signal to noise as a function of temperature, and doesn't broaden significantly as a function of pressure. This was a preferable pressure marker since it minimizes uncertainties in calculating pressure. The method for calibrating these pressure markers is interesting and worthwhile, but describing them in enough detail to do them justice could be its own thesis, and may lie outside of the scope of this work. Refer to Table 1 for more details on a selection of experiments in literature.

Resistive Heating Development

Conceptually, resistive heating might be viewed as simple. Materials have a certain resistance, R , which are a function of inherent properties coming from the resistivity, ρ , the length of the material, l , and the cross sectional area, A . This relationship can be shown with the equation $R = \rho \frac{l}{A}$. When some current is applied to the material of resistance, R , we get some power that can be used to heat, summarized by the equation $P = I^2R$. Resistive heating is common in both science and non-science industries, used as heating elements in kitchens and toasters as well as in high precision scientific ovens. Applying this technique to diamond anvil cell work gives rise to a number of considerations. For example, oxidation of the diamond anvil cell components must be considered, and so some groups perform their experiments under vacuum while some use a reducing gas environment. Some groups use a different diamond anvil cell material altogether to avoid oxidation of the cell [28].

Additionally, measurement of temperature becomes a critical component for success of a resistive heating experiment. Much of the literature discussion seems to consist of where the

thermocouple was placed and how much difference in temperature at different points of the sample. We note that even the most strategically placed thermocouple will likely give systematic errors compared to the absolute temperature of the sample, and thus it is advantageous to apply some other form of temperature measurement. We suggest the use of Raman Spectroscopy for an absolute measurement of temperature, and will discuss this in more detail in our methods section on the topic.

The table below includes a brief review of a few works using resistive heating from Jenei et al [28]. They highlight the variety of techniques employed to accomplish resistive heating experimentally as well as their pressure and temperature conditions reached. We note a wide variety in internal vs external heating as well as heating material used.

Table 2: Literature review of resistive heating experiments.

| Authors | Year | Temperature (°C) | Pressure | Heating | Type | Samples |
|--------------------------|------|------------------|------------------|-------------------------------|------|---|
| Boehler et al [29] | 1986 | < 1000 | <15 GPa | Fe wire | I | Fe (α - ϵ , α - γ), W |
| Schiferl [30] | 1987 | ~400—700 | 5-13 GPa | HT Oven-expensive (Re) | E | O ₂ |
| Basset et al [31] | 1993 | -190—1200 | ~2.5 GPa | Mo wire | E | H ₂ O, brucite, muscovite |
| Fei and Mao [32] | 1994 | ~700 | <86 GPa | Mo wire, inert gas flow | E | FeO |
| Dubrovinsky et al [33] | 1998 | ~1200 | <68 GPa | Graphite heater | E | Fe, Al ₂ O ₃ |
| Balzaretti et al [34] | 1999 | ~1100 | <4 GPa | Gasket heating (Re) | E/I | α -Si ₃ N ₄ , γ -Al ₂ O ₃ |
| Zha and Basset [35] | 2003 | ~2700 | <10 GPa (50 GPa) | Internal heating (Re) | I | SiO ₂ (Raman: qtz-coe) |
| Dubrovinskaia et al [36] | 2003 | ~1000 | <92 GPa | Whole-cell—special alloy cell | E | Fe _{0.95} Ni _{0.05} , TiO ₂ |
| Pasternak et al [37] | 2008 | ~1000 | 20 GPa | Small oven around diamonds | E | Ge |
| Weir et al [38] | 2009 | ~1700 | 21GPa | Internal resistive | I | Au |
| Weir et al [39] | 2012 | ~1700 | 45 GPa | Internal resistive | I | Sn |
| Du et al [40] | 2013 | 1027 | 50 GPa | Graphite ring | E | H ₂ O, Au |
| Jenei et al [28] | 2013 | 950 | 105 GPa | Dual mini heaters | E | CO ₂ , N ₂ |

Heaters for our experiments were made with a ceramic ring used as a guide for Nichrome-60 wires. The ceramic ring with wires was covered in high temperature cement and placed in a vacuum chamber to remove air. This process helped prevent weakening of the heater through oxidation. K-type thermocouples were created out of Alumel and Chromel wires and used with a standard thermocouple reader.

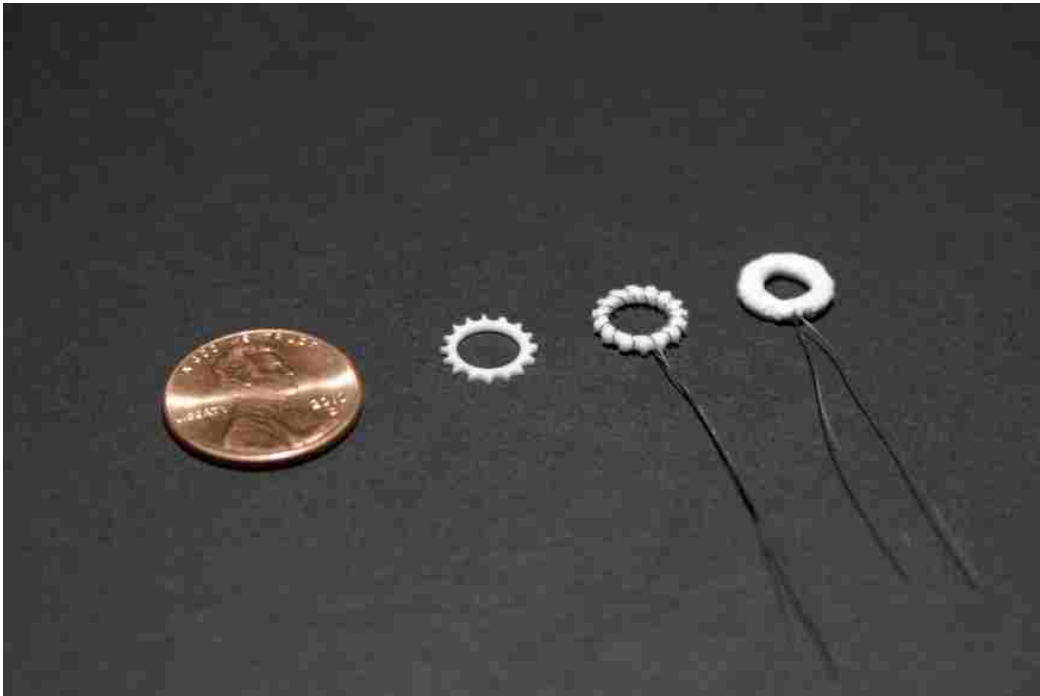


Figure 3: Stages of creation for the resistive heaters.

A huge instrumentation update for this set of experiments was to address the problem of a lack of thermal isolation; in other words, our heaters increased the temperature of the entire DAC and much heat was then lost to the environment. Our goal was to thermally isolate the heater-sample system as much as possible from the rest of the DAC, and our idea for reaching this goal was to create a thermally insulating backing plates. This way, although heat could still be lost through the diamonds and transferred to the backing plates, that the insulating backing plates would then transfer the heat to the rest of the DAC much less than the conducting WC backing plates.



Figure 4: Diamond anvil cell with ceramic backing plates used in a resistive heating experiment.

We machined our seats out of un-sintered ZrO_2 , taking results of a DAC made entirely of the same material as proof of concept [41]. The first geometry of our designs was simply two ceramic cylinders with 1.5mm diameter holes through the center.

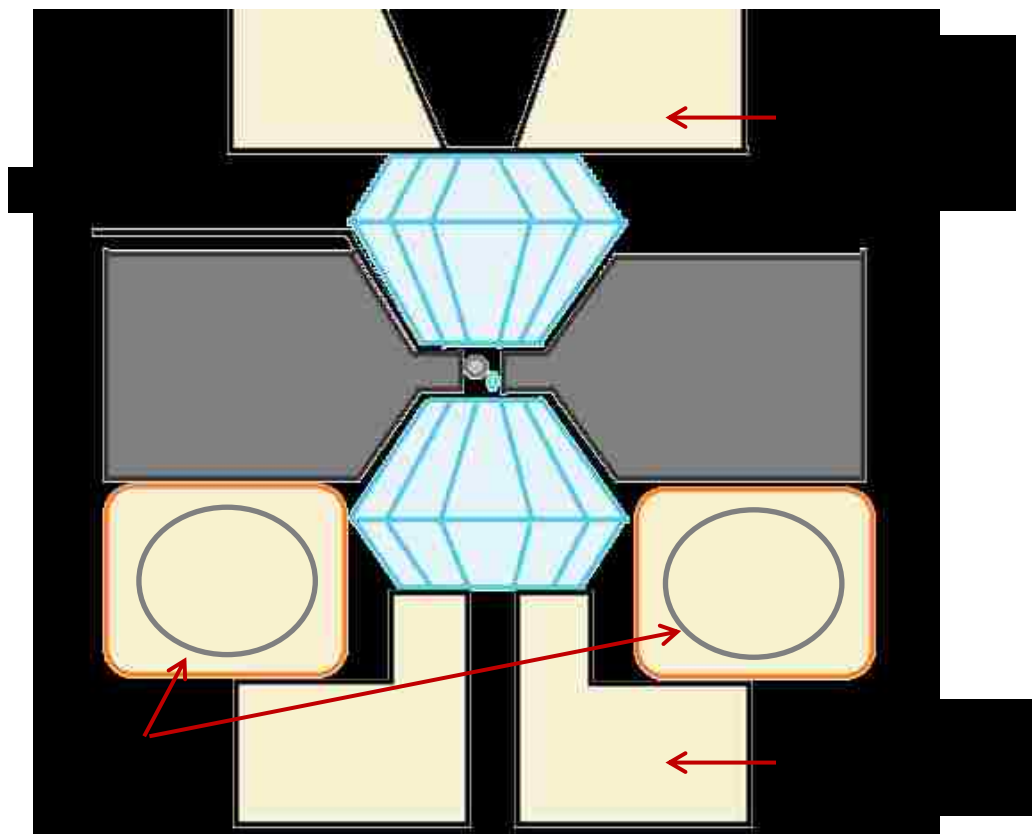


Figure 5: Annotated cross sectional diagram of the resistive heating diamond anvil cell setup

Raman Spectroscopy

Raman spectroscopy is an inelastic scattering technique that uses monochromatic laser light to observe the molecular vibrations, phonons, or other excitations in a lattice. The incoming light excites the system to virtual excited states, providing a change in momentum that is often recorded as a change in frequency from the excitation wavelength. These frequency shifts are often reported in units of relative cm^{-1} with the excitation wavelength representing 0 cm^{-1} ; much of the incoming light is elastically scattered and is called Rayleigh scattering. A shift to lower frequency is called an Anti-Stokes mode, and a shift to higher change frequency is called a Stokes mode. A Stokes mode is a transition from a lower energy state to a higher one, and an Anti-Stokes mode is a transition from a higher energy state to a lower energy state. At ambient temperatures, the population of lower energy states will be higher and thus the Stokes modes will have higher intensity than Anti-Stokes. The intensity of the Anti-Stokes peaks will increase with temperature as the population of higher energy states increases. The number of allowed Raman modes in the spectrum depends heavily on the crystal symmetry and the strength of strength of intermolecular bonds [42].

Using Boltzmann statistics, we follow the derivation given in [42] to get a relationship between temperature and the intensities of the Stokes vs Anti-Stokes modes. Equation 4.36 on page 84 gives the following

$$\frac{I_s}{I_a} = \frac{(\nu_0 - \nu_k)^4}{(\nu_0 + \nu_k)^4} \exp\{hc\nu_k/k_B T\}$$

where (I_s) is the intensity of the Stokes mode, (I_a) is the intensity of the Anti-Stokes mode, ν_0 is the wavenumber of the Rayleigh scattered light, ν_k is the wavenumber of the k^{th} Raman mode, h is Planck's constant, c is the speed of light, k_B is Boltzmann's constant and T is temperature.

By rearranging this equation to isolate temperature, T, we get

$$T = \frac{hc\nu_k}{k_B \left[4 \ln \left(\frac{\nu_0 + \nu_k}{\nu_0 - \nu_k} \right) + \ln \left(\frac{I_s}{I_a} \right) \right]}$$

We can use this relationship to calculate the absolute temperature of the sample.

The ratio of the intensities of Stokes vs Anti-Stokes will come to unity faster for modes close in frequency to the Rayleigh line than for modes farther away. Additionally, some samples are not Raman active or have phases that are not Raman active, and thus for those samples temperature could not be determined using this method. We propose the notion of a Raman “temperature marker”—a system that allows modes spaced at a variety of frequencies. For the experiments listed in the Case Studies—Sn section, we used CaCO₃ as a temperature marker because of its decent spacing of modes from 0—1000 cm⁻¹ and its high melting temperature compared to tin.

Case Studies

This case studies section is somewhat chronological in time, and somewhat organized by topic. Work with the simple organic systems of glycine and aspirin is discussed first, followed by our work mapping the β -tin phase boundary. Work with Lawrence Livermore National Lab on related glycine work and the application of resistive heating for connected or ongoing lab projects is also briefly described.

The Resistive Heating Story:

Glycine Results

Glycine has many polymorphs that have been extensively studied both under ambient and high pressure conditions[43]–[46]. It is the simplest amino acid and has many practical uses in science and industry. Glycine’s selection as our first sample came from glycine’s low melting temperature, ~233C, and its existing polymorphism[47], [48] indicating a rich energy landscape.

Synthesis of existing ambient pressure polymorphs was the first attempted step. Following the procedures given in [49]and [47] for β -glycine and γ -glycine respectively, β -glycine crystals were successfully synthesized, but attempts at crystallizing pure γ -glycine were unsuccessful. The polymorphic structure was confirmed by comparing collected Raman Spectroscopy data with literature and by visually inspecting the morphology of synthesized crystals.

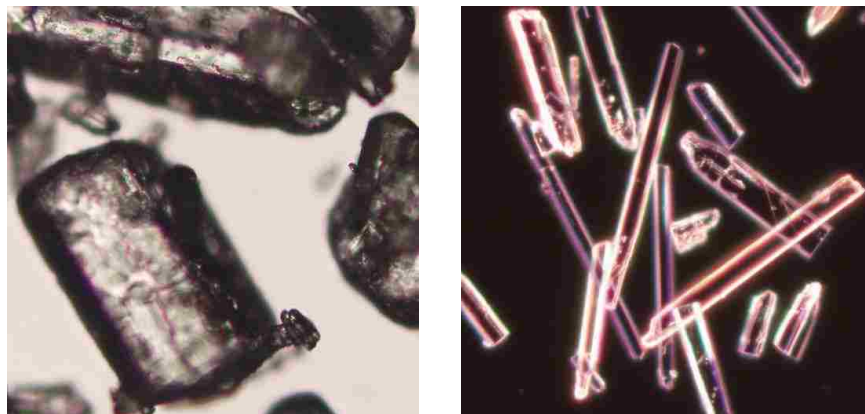


Figure 6: Comparison of glycine polymorph morphologies. A) α -glycine and B) β -glycine

Early in the exploration of simple organics, our instrumentation for resistive heating was still under development. Outside of the DAC, the first generation heater had a max temperature of about 800C. Even considering thermal loss to the other elements of the DAC, the melting temperature of glycine certainly seemed within reach. For glycine, our thermometry was also still

in its first stages of development. A thermocouple was placed on the gasket but not near the sample, and a second thermocouple was placed on the back of the diamond with the heater on it. Glycine was loaded with no pressure transmitting medium in the sample chamber. The Raman spectra were recorded from the sample as function of temperature using an Andor spectrometer.

At about 1 GPa, when glycine was heated past its reported ambient temperature melting point, two observations were made: 1) as temperature increased, the intensity of the Raman spectra decreased until at a certain point it disappeared completely, and 2) well past the ambient pressure melting point in temperature, our sample experienced what we suspected to be decomposition based on the Raman spectra which looked like amorphous carbon. Pressure was not recorded *in situ* during the experiment, only before and after heating experiments. Based on later experiments, it's likely that pressure fluctuated during the heating, but this was not measured at the time. Below a stack plot of the results are shown.

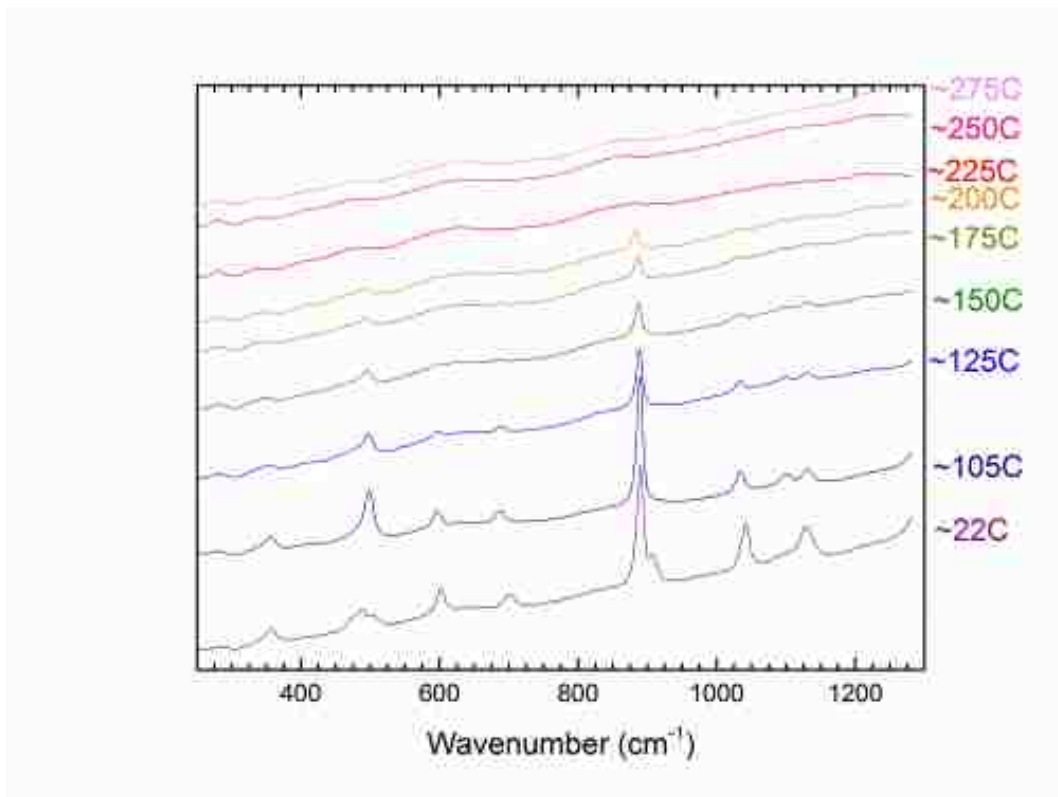


Figure 7: Raman stack plot of glycine as a function of temperature.

Glycine was heated at about 5 GPa in another experiment with no PTM. At this point, a second generation of heaters was in use. The second generation heaters have more wire turns meaning that the same temperature could be achieved with less power and potentially a higher maximum temperature could be achieved. In this experiment, the Raman modes observed for glycine were already gone at a much lower temperature than expected. The switch to a more powerful heater without an improvement to the thermometry at the time could have played a role in this earlier disappearance. When the temperature was increased in search of any visual indications of melting, the sample over time became opaque which appeared to indicate decomposition. The opacity increase of the sample is shown below.

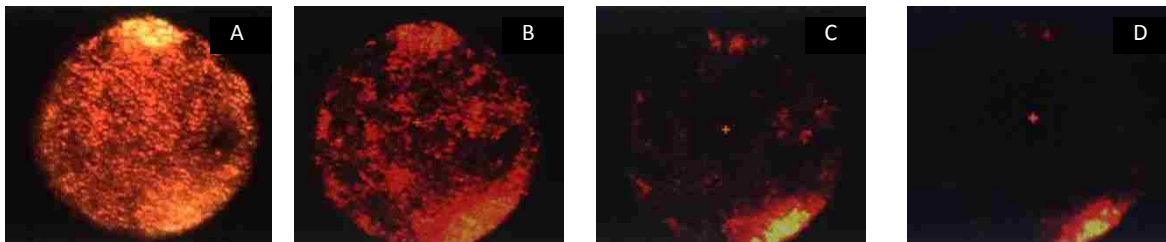


Figure 8: Glycine turning opaque as temperature increases (A to D). Transmission lighting geometry used.

Since the resistive heating method was not as well developed at the time and many concerns arose surrounding this, attempting to melt glycine at ambient pressures outside of the DAC seemed to be the most prudent step. When trying to observe visual evidence of melting glycine, the sample turned amorphous well before the reported melting temperature. When the experiment was repeated while collecting Raman, it seemed yet again that the sample had a very narrow range in temperature between potentially melting to decomposing even at ambient pressures. This window was too narrow for the early capabilities of our resistive heating

configuration at that point and decided to move on to another sample to continue to build the method.

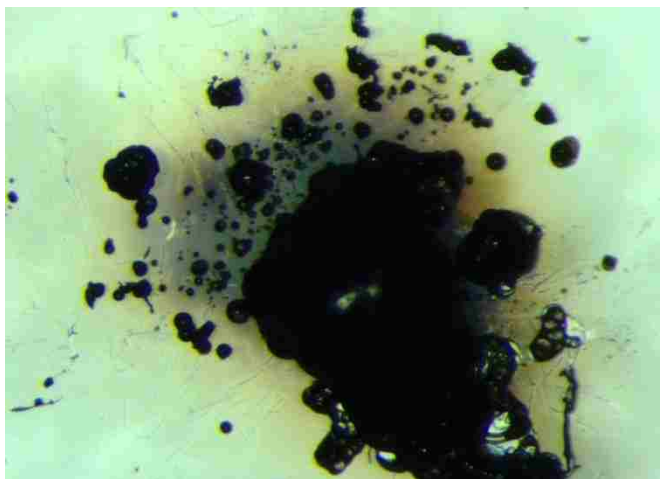


Figure 9: Glycine heated at ambient pressures on glass slide (no cover slide) to 230C.

Glycine ambient P heating between glass slides on Hot Plate

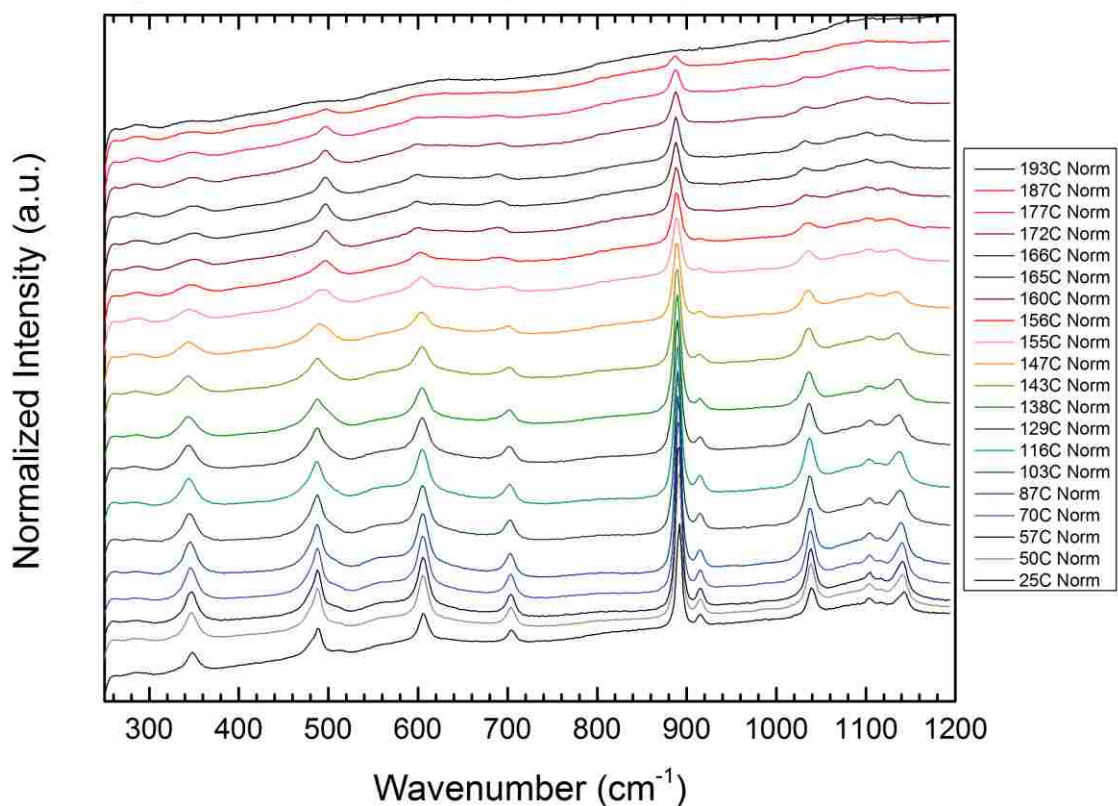


Figure 10: Raman stack plot of glycine as a function of temperature. After disappearing well before the reported temperatures, the Raman modes never fully returned.

These early resistive heating experiments with glycine gave an infrastructure for imposing standards and criteria for future experiments. Tracking pressure during heating to account for changes became one of the first standards. These experiments showed how critical accurate measurement of temperature is—thermocouple placement close to the sample became another standard for future experiments. A sample that definitely melted at ambient temperatures became another standard for future experiments. This last restriction led to Aspirin as the next sample to study.

Aspirin Results

Aspirin displays polymorphism, but it has fewer known polymorphic forms than glycine does [8], [50]–[52]. It also has an ambient pressure melt phase measured by Shtukenberg et al [8], which we confirmed visually before proceeding with this sample.

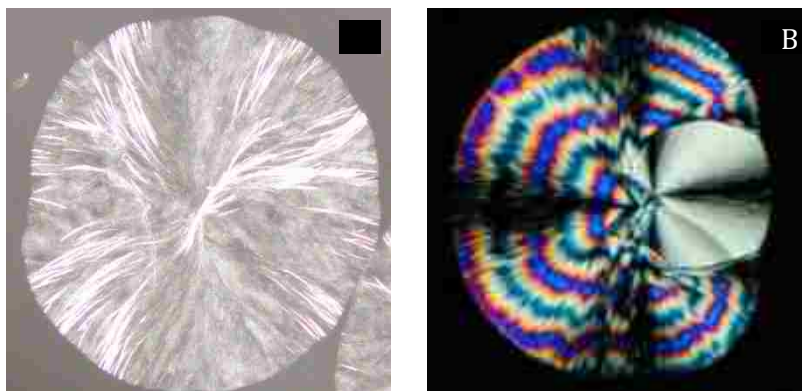


Figure 11: Melt product of aspirin. A) Melt product observed in our lab. B) Spherulite melt product of aspirin-IV measured by Shtukenberg et al

We note that we did not measure the Raman modes of Aspirin-IV, and only confirmed melting visually and with the general morphology reported. Based on the complications of measuring the short lived phase IV[8], it seemed sufficient at the time to observe the visual changes to aspirin as a function of temperature across its melt line at ambient pressures.

The first DAC loading of aspirin-I was loaded with ground aspirin from Sigma-Aldrich and no PTM, and included a Sm:YAG crystal as a pressure marker. Each high-temperature Raman measurement was accompanied by a measurement of the pressure marker throughout the experiment. During the heating, a shift in the Raman frequencies at high temperatures was observed; however, it turned out to be a shift due to pressure loss rather than temperature.

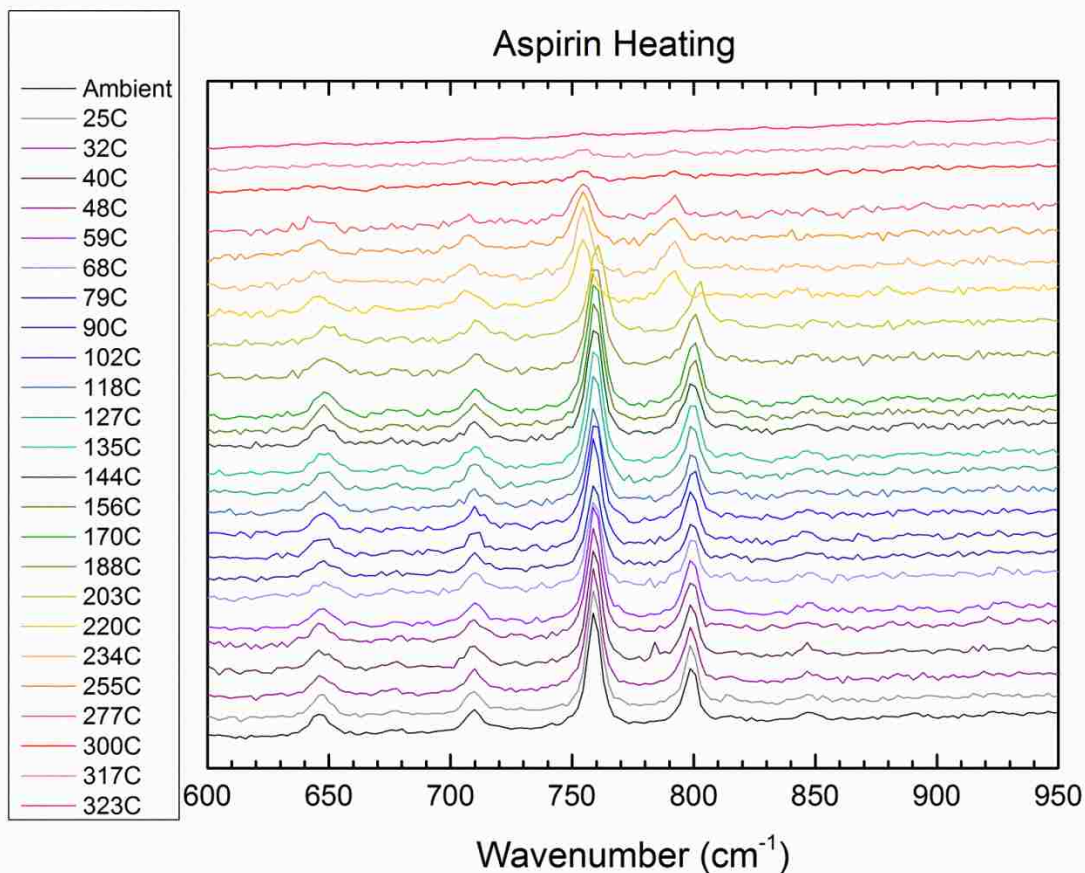


Figure 12: Raman stack plot of a small selection of aspirin modes. Between ~ 200 - 220C , a negative shift in frequency is observed. This is due to a loss of pressure (known because of Sm:YAG pressure Data) rather than due to temperature.

At this point, two problems needed to be addressed; firstly, the DAC relaxing under high temperature conditions, and secondly, in the ambient spectrum of aspirin, some peaks not identified in literature were present. In other words, sample purity was a concern. Let us consider this issue first. In the sample purchased from sigma Aldrich, spurious modes were present in the spectra that weren't present in modes published in the literature. Thinking that this may be an issue of purity, we aimed to try creating single crystals of the material which would be inherently pure. A few attempts were made by simply making an oversaturated solution and then allowing it

to crystallize by slow evaporation. The first batch was unsuccessful, showing almost the same result as the original sample. The second batch gave spectra that matched the literature better but still had one or two spurious peaks. Our Lawrence Livermore National Lab (LLNL) collaborator, Natalia Zaitseva, provided us with a few particularly large single crystals [53]. The same spurious peaks were observed in the Raman spectra of a set of single crystals of LLNL Aspirin. Identifying these peaks would be the goal of a future date, but for the moment, it was part of the characterization of our sample. We moved forward with tracking the modes we could see whether or not they belonged purely to ASA-I.

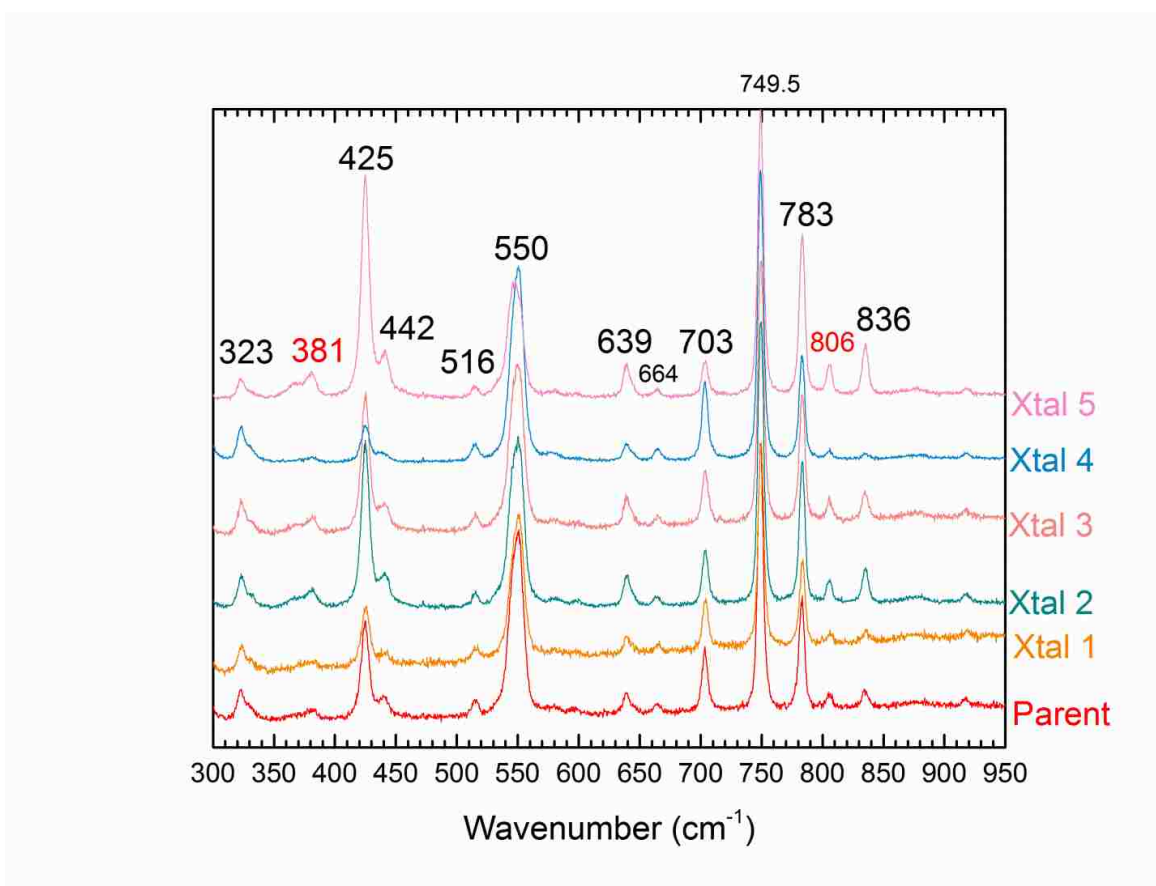


Figure 13: Raman stack plot of a set of crystals grown from slow evaporation. Only selection of the modes of aspirin phase I are shown here. Modes labeled in red did not appear in literature.

As for addressing the problem of the DAC relaxing, several solutions were apparent. Larger culet diamonds would require more force to apply a lower pressure. This would mean that although the DAC could relax the same amount, not as much pressure would be lost during the heating. A gas membrane to apply pressure rather than pressure screws could also be a solution. The concept for gas membranes as used for diamond anvil cell is described in many cases in literature, and we give [54] as an reference here. As the temperature increased, if pressure changed in the DAC due to heating, the membrane pressure could be used to compensate. Lubricating the outside of the piston and the inside of the cylinder pieces of the DAC was also considered—a technique commonly applied in mechanics and engineering to metal or other materials heating up so that the system behaves optimally. Our final idea centered on addressing the issue of the DAC being heated at all. Other groups use a different material for the DAC itself, such as Inconel [28], so that the thermal expansion of the material is low and pressure loss would be less likely when the DAC material inevitably heats. As discussed in the methods section, our idea was to prevent the entire DAC from heating up in the first place. For Aspirin, the first two techniques were applied for different experiments. Lubrication has not been attempted yet. The final solution proved to be a huge jump in successful instrumentation, and is described in the Resistive Heating Methods Section as well as mentioned in the Case Studies β -Sn section.

The second DAC loading of Aspirin-I used powdered LLNL single crystal non-hydrostatically loaded with no PTM. The gas membrane was employed to control the pressure loss issue described above. The Raman modes under pressure and temperature were observed while heating and when the Raman modes disappeared at temperature, the temperature was immediately decrease and cooling data was taken. The sample was heated and cooled six times under various pressure and temperature conditions. Our results are summarized in the graph below. We identified the Raman modes to be consistent with existing phases within the regions we studied and did not see any new phases appear.

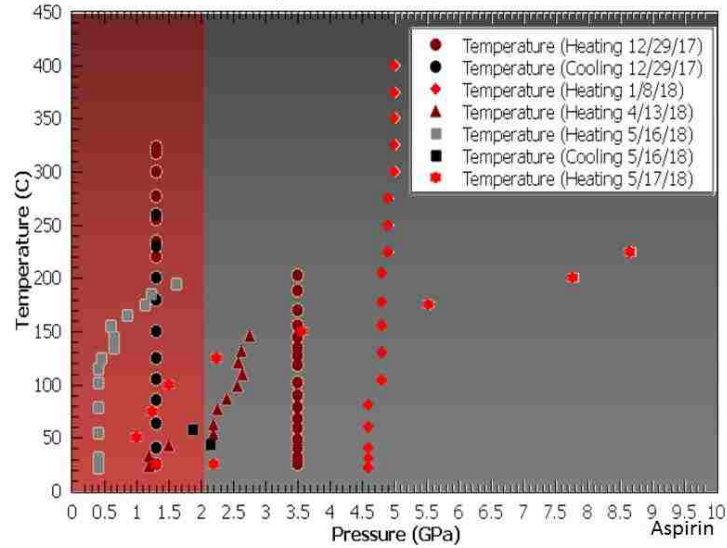


Figure 14: Mapping of where Raman spectra were taken for aspirin in phase space. Points with the same shape indicate the same temperature cycle. Points found in the red region were identified as phase I while points in the grey region were identified as phase III.

Visual observation of aspirin melting at pressure in a DAC had not yet occurred. Thus, the final loading of aspirin-I used a small LLNL single crystal loaded in an Ar PTM with a Sm:YAG pressure marker in search of visual evidence of melting. Larger culet diamonds were used to address the pressure loss issue in a different way as discussed above. The starting pressure for the sample was above 5 GPa since we had lost pressure in earlier resistive heating experiments below this starting pressure with no gas membrane. The Raman modes of aspirin were recorded until they disappeared, and then the sample was monitored visually with increasing temperature hoping to see the sample change morphology in some way to indicate melting. No morphological changes were observed during this process. The sample did turn dark beyond a certain temperature and this indicated decomposition much like glycine had experienced.

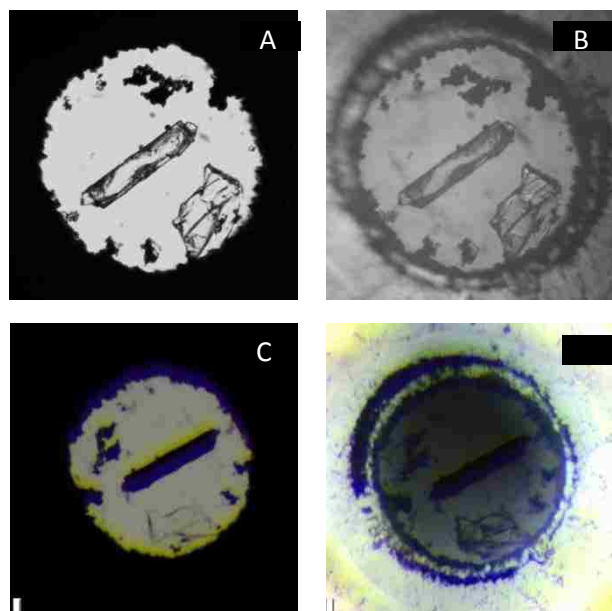


Figure 15: Single crystal of aspirin phase I in an Ar PTM with Sm: YAG crystal loaded in DAC. A) and C) are transmission lighting geometry while B and D are reflected lighting geometry. A) and B) are before heating while C) and D) are after heating. The sample becomes opaque when heated.

Our uncertainties about our technique were too many for us to rule out what was or wasn't working with simple organic systems such that a more robust sample seemed necessary.

Simple Organics Discussion

Although we moved away from simple organic systems for the time being, we have some questions and strategies for moving forward for either our future selves or the interested reader hoping to pursue this topic someday. The first real hurdle to overcome is to define criteria theoretically for what should happen to the Raman spectra when the sample melts. If melting is defined to be the loss of strong intramolecular bonds in a crystal, then spectra from the individual molecules and the covalent bonds keeping them together might still be expected. For example, for glycine dissolved in water, a Raman spectrum is still observable despite the individual molecules

being separate in zwitterion form [55]. This is because Raman spectroscopy not only probes lattice modes in a crystal, but also vibrational and rotational modes of molecules which wouldn't necessarily disappear under melt conditions. We did not observe this phenomenon when heating our organic systems though, only the loss of all modes at a particular temperature. It's possible that the window between decomposition and melting for these materials is too small for our current capabilities. For now, we can't give or find a satisfactory answer for this complex behavior we observe. It's possible that an additional diagnostic technique for describing melt criteria in simple organic systems is necessary, although techniques used for metals such as pyrometry using the reflectivity of the metals seems difficult to apply at first glance.

If we were able to define these criteria and identify a sample that could follow those criteria, our next step would be to apply pressures that are exceptionally low initially. If indeed we could ensure that our sample melts at a particular temperature, we would begin by applying the lowest pressure possible initially. In simple organic crystals, when applying pressure, the sample's density will increase and this is usually the bonds between the molecules in the crystal becoming shorter and therefore stronger. This could increase the melting temperature, and it's possible that the increase would be dramatic. Is it possible that we may have been missing the window for melting entirely by beginning our search for melting at 5-10 GPa? No one really seems to know the answers to these questions because no one has really applied this technique to these systems before as far as we could tell as in literature, a melt curve or phase diagram for these systems seems to be non-existent.

β -Sn Results

Without visual evidence of melting of any samples and looking for a more robust system less prone to decomposition, we moved to consider a simpler metallic system. A system with a low melting point and rich polymorphism was still ideal, but requirement that the sample not decompose proved necessary to add. We were inspired to look at tin based on our familiarity of dealing with the system in the past and based on how well it has been studied in order to give a better baseline to compare to for our obtained results.

Tin has been in use for a long period of history, and remains ubiquitous in industry today. Popular urban legends involving tin include Napoleon's soldiers' tin buttons crumbling in the frigid Russian winter [56], or concern arising that some nefarious evil was at work when tin church organ pipes warped over many chilly winters [57]. Colloquially, this phenomenon is referred to as tin pest, and scientifically, tin is known to have a volume expanding β — α transition at low temperatures [57], [58]. Of particular interest is tin's behavior at extreme conditions such as high pressure and high temperature. Tin's phase diagram is extremely well studied, especially its melt curve under pressure [10], [59]–[61]. Although the melt curve of tin has been mapped extensively to very high pressures, the phase stability of β -Sn to bct-Sn transition has only been extrapolated and not explicitly measured. Tin proved to be the ideal system observing interesting physics and displaying the strength of the method we developed.

Literature for Raman spectra of tin is limited—only one paper total claimed to see the Raman modes of tin at low temperatures [62]. There are two allowed Raman modes of β -tin— B_{1g} and E_g , calculated using selection rules from structure. Choosing space group 141 for β -tin's $I4_1/amd$ structure and 4a Wyckoff position (0, 0, 0) showed two allowed Raman modes [63]. A back of the envelope calculation using this information and the phonon density of states [64], [65] revealed that modes should roughly be present at around 50 cm^{-1} and 140 cm^{-1} . The Raman modes

of tin were preliminarily observed in a diamond anvil cell with NaCl PTM and Sm: YAG pressure marker and is shown in the figure below, which has the modes approximately where our rough estimation predicted. Although reference [62] claimed to produce the first Raman spectra of tin, their spectra was not well resolved close to the Rayleigh line. Our experiments are the first to clearly show both allowed modes of β -tin.

The attempts to visually observe melting of a sample in a DAC continued with tin. Implementation of the ceramic backing plates described in the Resistive Heating Methods section greatly improved heat transfer to the sample in the following experiments and allowed a new maximum temperature to be recorded inside the DAC ($\sim 715\text{C}$). The sample was loosely packed with a KBr PTM, and the DAC was only closed with no pressure. As the sample was heated, we observed the sample moving about in the sample chamber. Morphological visual changes in a sample in a resistively heated DAC had finally been shown.

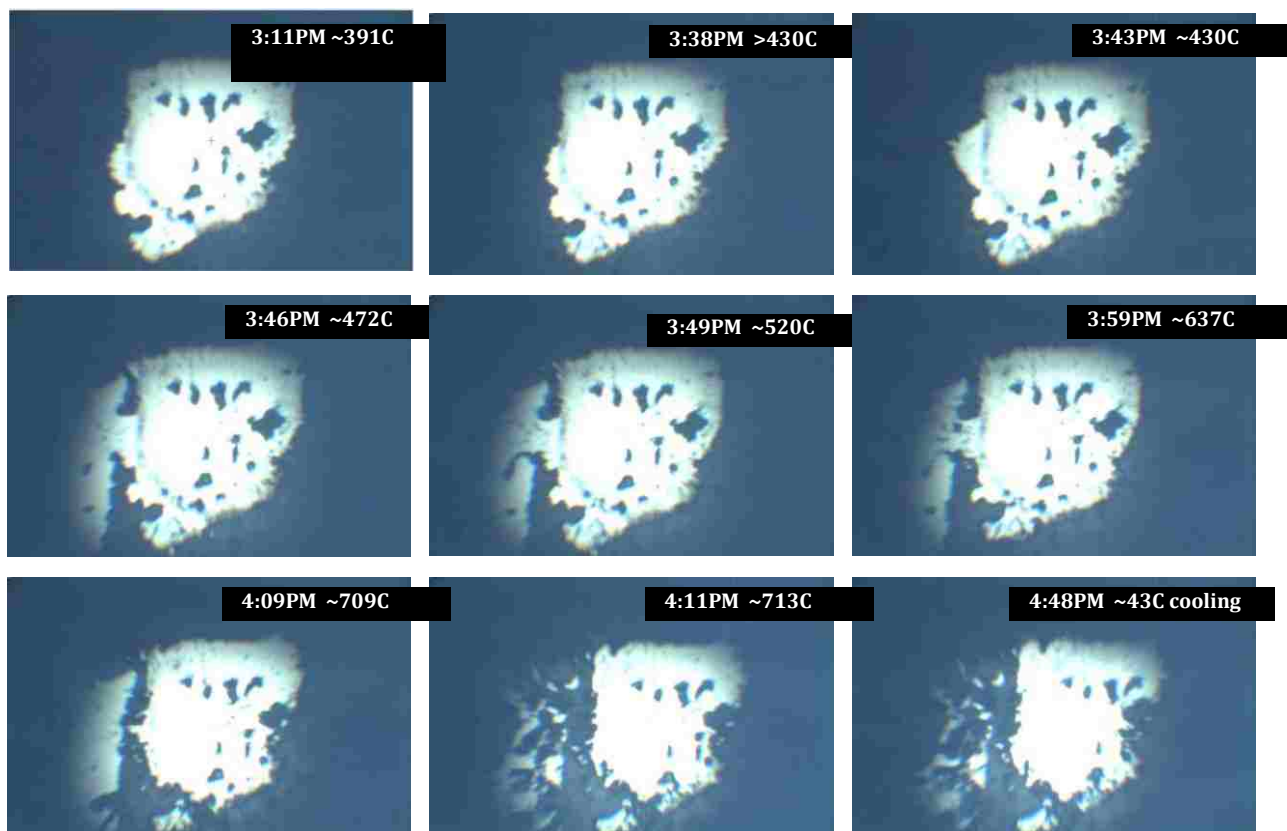


Figure 16: Tin in diamond anvil cell showing visual evidence of melting as a function of temperature and time.

This is a somewhat surprising result. Usually, some kind of change obvious to the naked eye is not present when heating samples, which is why techniques such as speckle measurement where temperature gradients are needed for the material to flow. Since, in DAC experiments, the PTM presses on the sample from all directions and using resistive heating we are in a steady state, it's unlikely that anything visible to the human eye will be observed.

Although changes to the sample were observed indicating melting, the Raman spectra from this experiment were poor due to the small collection angle provided by the 1.3mm diameter hole in the ceramic backing plate. With a modification to the cylindrical ceramic backing plate to have a larger angle opening, we were able to collect high quality spectra once again. We also note that at

this point we began to use $\text{SrB}_4\text{O}_7:\text{Sm}^{2+}$ as a pressure marker. With confirmation of melting done, we began our investigation into the phase boundary of β -Sn using literature values as a rough reference for where phase boundaries should be, approaching those boundaries slowly in temperature.

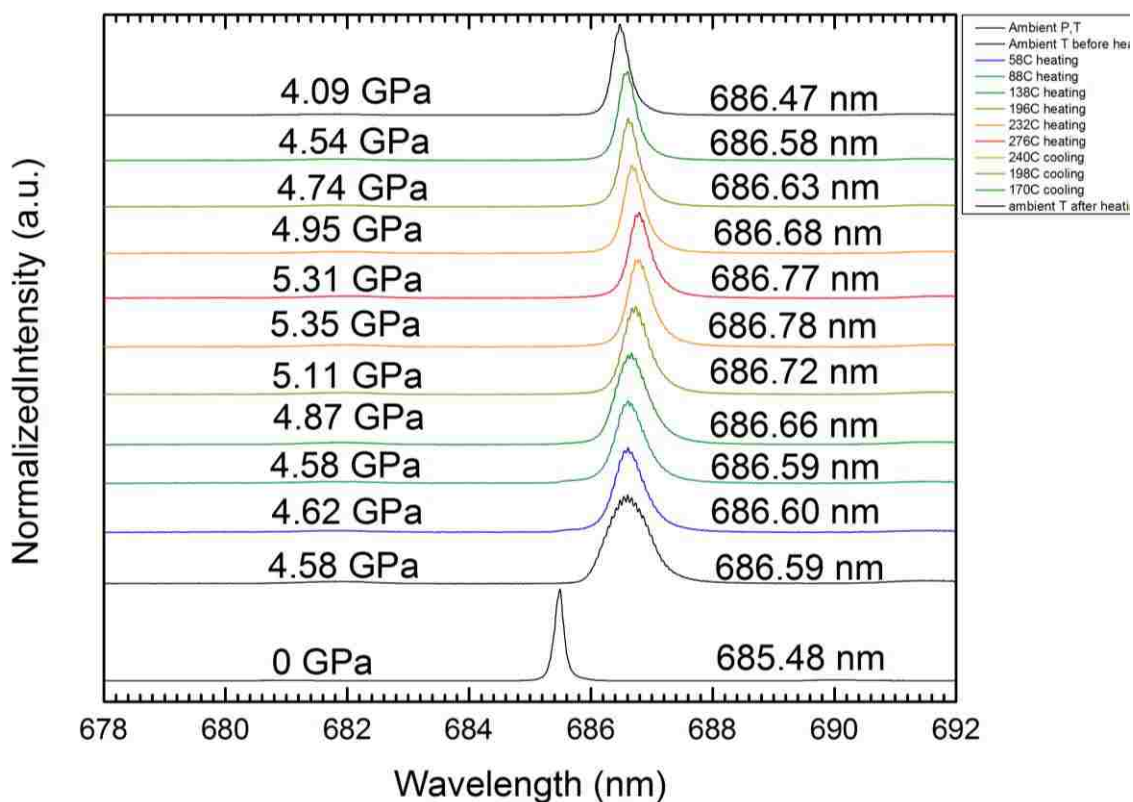


Figure 17: $\text{SrB}_4\text{O}_7:\text{Sm}^{2+}$ fluorescence spectra stack plot as a function of temperature.

We track the Raman modes of tin until they disappear. As we approach the β -Sn melt phase boundary, the modes experience a gradual loss of intensity. When crossing the β -Sn to bct-Sn phase boundary, we observe a sudden and complete loss of all Raman modes. We record one or two points past where the Raman disappears, and observe hysteresis in the reappearance of Raman across the β -Sn to bct-Sn phase boundary.

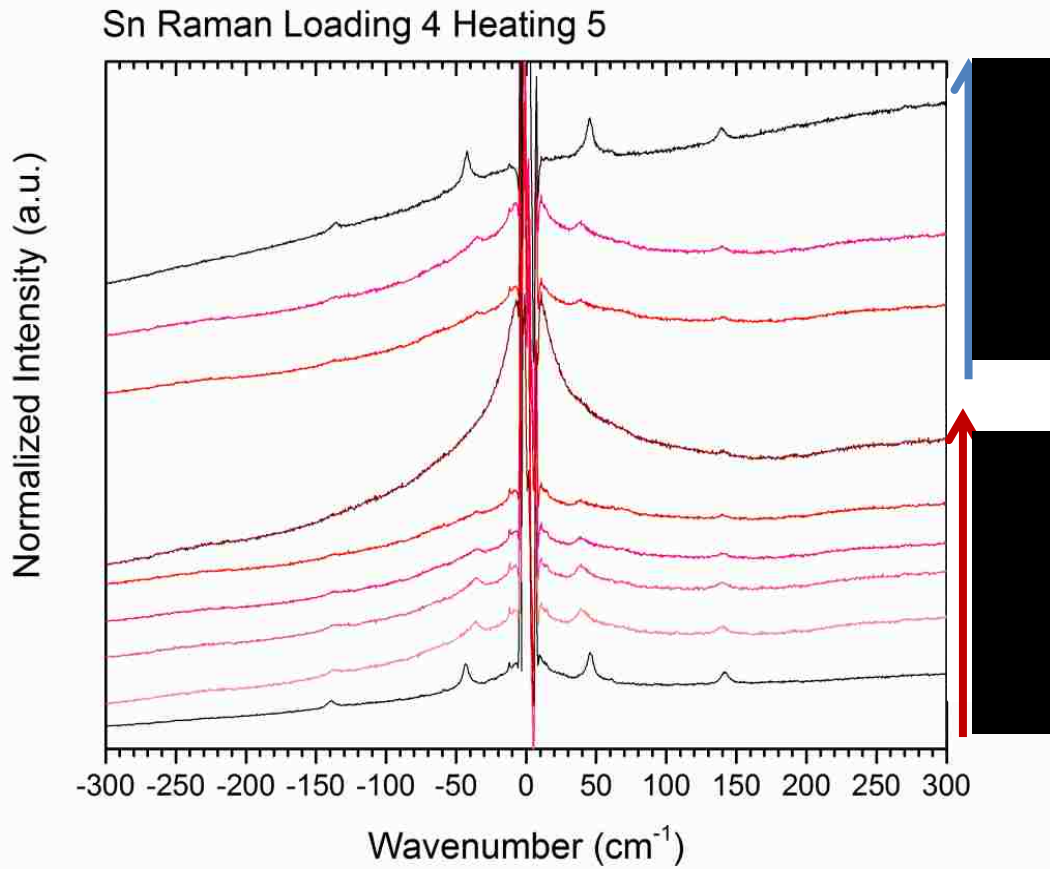


Figure 18: Raman spectroscopy stack plot of tin as a function of temperature across melt boundary.

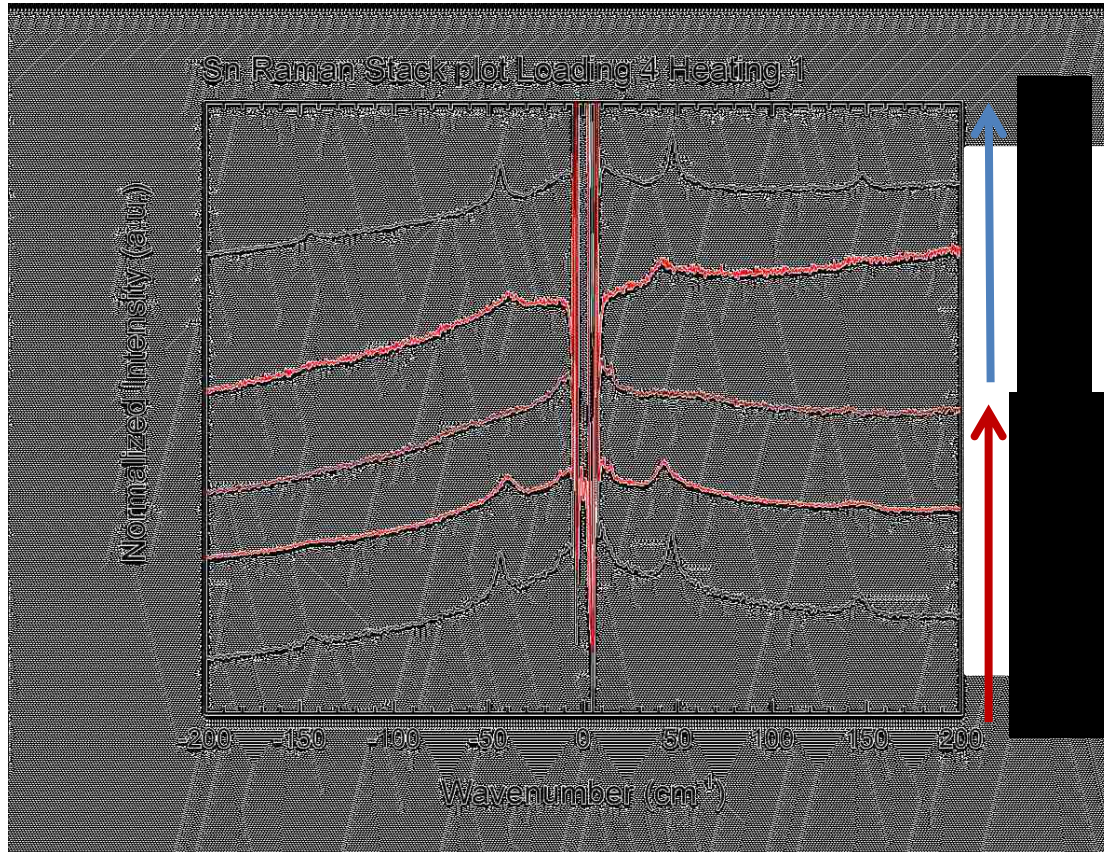


Figure 19: Raman spectroscopy stack plot of tin as a function of temperature across a solid-solid phase boundary.

β -Sn Discussion

β -Sn has the structure $I4_1/amd$ which is a disordered body-centered tetragonal structure. It has two atoms in its primitive unit cell which allows for optical phonons. Two Raman modes are allowed for β -Sn: B_{1g} and E_g . When crossing the melt phase boundary, the modes for β -Sn broaden out with the increase of temperature until disappearing. When crossing the β -Sn to bct-Sn, we observed a sudden loss of modes observed. Bct-Sn is also body-centered tetragonal, but slightly more ordered; the structure for bct-Sn is $I4/mmm$, and it has only one atom in its primitive unit cell. Thus, no optical phonons are present and no Raman modes are allowed in this region of the phase diagram.

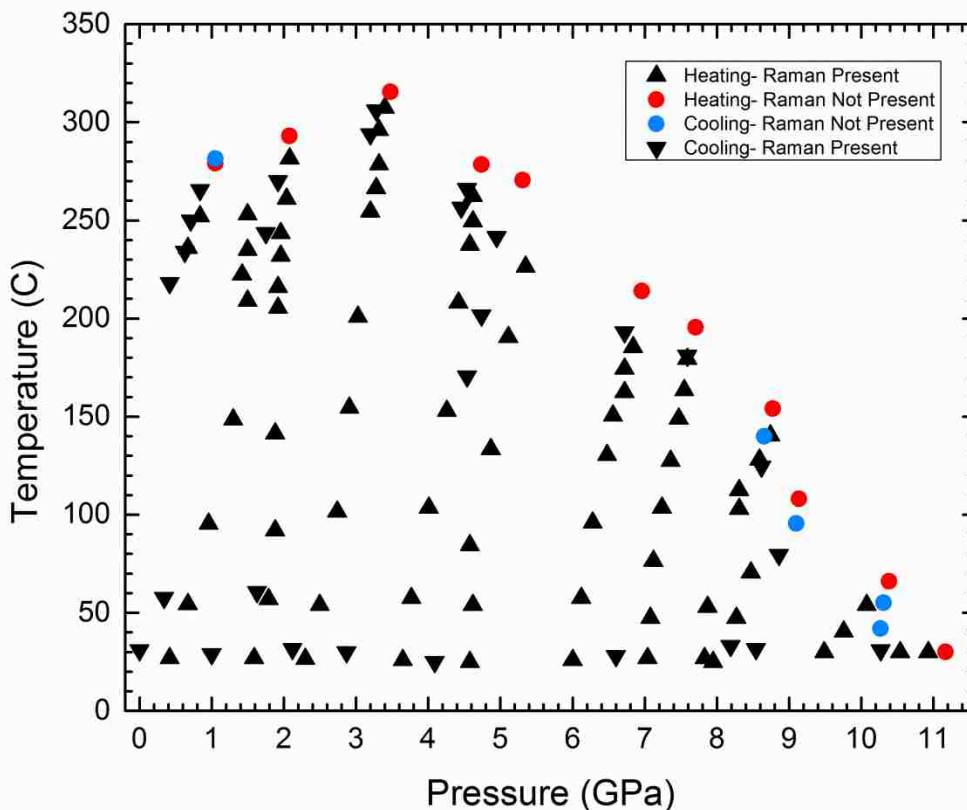


Figure 20: Phase diagram mapping the phase stability of β -Sn

The above phase diagram reports temperatures from our thermocouple, which was placed on the between the culet of the diamond and the indent of the gasket. We plan to calculate temperature directly using the formula listed in our Raman Spectroscopy Methods section; however, since the Raman modes of tin have frequencies close to the Rayleigh line, the intensities of the stokes vs anti-stokes will come to unity rather quickly in temperature. We employed a Raman “temperature marker” that has modes at a much wider range of frequencies to help us corroborate the temperatures we will calculate from Sn and the temperatures our thermocouple reported. We chose CaCO_3 for this experiment because of its modes at a good range of frequencies and its

abundance and availability. In future experiments, we will probably try different Raman temperature markers.

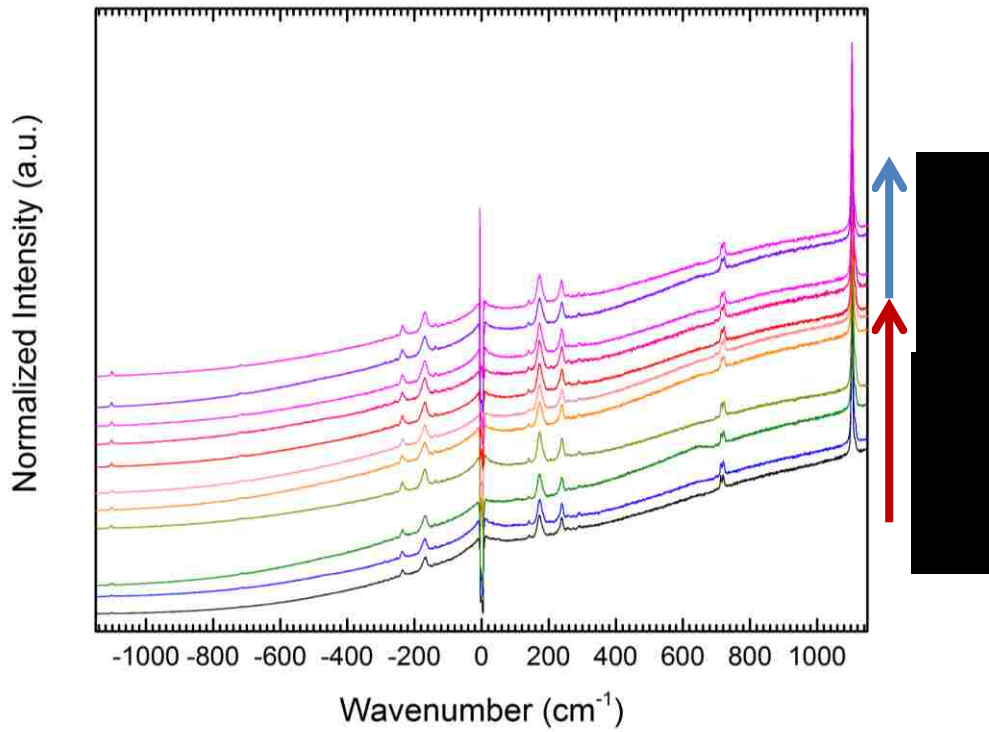


Figure 21: Raman stack plot of CaCO₃ as a function of temperature. The ratios of the Stokes to Anti-Stokes intensities of a mode can be used to calculate absolute temperature.

As mentioned earlier, in order to complete the temperature calculations, we need to perform a transfer function for our Raman system. The transfer function is a calibration of the quantum efficiency of the CCD in the spectrometer system. The calibration would allow the intensities of each Raman mode taken as a true and absolute intensity.

Related Work:

α -glycine EOS and Raman

Our first highlighted work came from our initial interest in glycine was our collaboration with Lawrence Livermore National Lab working with Dr. Elissaios Stavrou, wherein we studied the structural stability of α -glycine under pressure [66]. In this work, α -glycine crystal structure was measured with X-ray diffraction (XRD) and subtle changes to the vibrational modes were measured with Raman up to 50 GPa, and the room temperature equation of state (EOS) was determined. In addition to our experimental work, several calculations techniques were applied including vibrational calculations to extract the positions of the allowed Raman modes and intensities, and theoretical EOSs. This work is arguably one of the most thorough and highest static pressure studies of glycine to date.

Resistive heating at HPCAT

Beyond the author's individual projects, we applied resistive heating to previous and ongoing projects involving time at Argonne National Lab at the Advance Photon Source (APS) HPCAT beamlines. We highlight our published work on Sn_3N_4 [67] where the main contribution from resistive heating was that heating our sample at a slower rate provided different results than our laser heated samples and allowed us to match theoretical work better. We also mention here our work with resistive heating using XAFS. In many ways a proof of concept work, the data from this project is still being analyzed and will be in press for publication soon.

Conclusions

The phase stability of β -Sn as a function of pressure and temperature has been measured using Raman spectroscopy and a resistively heated diamond anvil cell; this is the first phase mapping of a metal using Raman spectroscopy. The difference between melt transitions and first-order solid-solid phase transitions are distinguished in this thesis. The strength of using Raman as a route to absolute temperature measurement was discussed and excellent data quality for Raman spectroscopy of metals has been displayed. This thesis shows that thermal isolation can prove essential to performing a successful resistive heating experiment. It also shows that visual evidence of melting is too qualitative of a criterion and that more quantitative methods such as spectroscopy (i.e. Raman) are more ideal for developing melt criteria. Careful sample selection was shown to be critical for the success of this technique— some systems are not well suited to resistive heating diamond anvil cell experiments. The technique described in this work is ideal for measuring metallic systems with either debated or controversial phase boundaries. Lithium, bismuth, and silicon all have interesting phase diagrams with Raman active phases and high temperature regions that would be ideal to apply this technique to.

References

- [1] J. S. Schilling, "The use of high pressure in basic, materials, and life sciences," *Hyperfine Interact.*, vol. 128, no. 1–3, pp. 3–27, 2000.
- [2] C. Childs *et al.*, "Covalency is Frustrating: La₂Sn₂O₇ and the Nature of Bonding in Pyrochlores under High Pressure-Temperature Conditions," *Inorg. Chem.*, vol. 57, no. 24, pp. 15051–15061, 2018.
- [3] A. M. J. Schaeffer, W. B. Talmadge, S. R. Temple, and S. Deemyad, "High pressure melting of lithium," *Phys. Rev. Lett.*, vol. 109, p. 185702, 2012.
- [4] Q. Zhu *et al.*, "Resorcinol Crystallization from the Melt: A New Ambient Phase and New 'Riddles,'" *J. Am. Chem. Soc.*, vol. 138, no. 14, pp. 4881–4889, 2016.
- [5] L. O. Hedges and S. Whitelam, "Limit of validity of Ostwald's rule of stages in a statistical mechanical model of crystallization," pp. 1–6.
- [6] J. Nyvlt, "The Ostwald Rule of Stages," *Cryst.Res.Technol.*, vol. 30, no. 4, pp. 443–449, 1995.
- [7] J. Halebian and W. McCrone, "Pharmaceutical Applications of Polymorphism," *J. Pharm. Sci.*, vol. 58, no. 8, pp. 911–929, 1969.
- [8] A. G. Shtukenberg *et al.*, "The Third Ambient Aspirin Polymorph," *Cryst. Growth Des.*, vol. 17, no. 6, pp. 3562–3566, 2017.
- [9] A. R. Oganov, C. J. Pickard, Q. Zhu, and R. J. Needs, "Structure prediction drives materials discovery," *Nat. Rev. Mater.*, 2019.
- [10] R. Briggs *et al.*, "High-pressure melting behavior of tin up to 105 GPa," *Phys. Rev. B*, vol. 95, no. 5, pp. 1–8, 2017.
- [11] A. Jayaraman, "Diamond anvil cell and high-pressure physical investigations," *Rev. Mod. Phys.*, vol. 55, no. 1, pp. 65–108, 1983.
- [12] P. W. Bridgman, "Compressions and polymorphic transitions of seventeen elements to 100,000 kg/cm²," *Phys. Rev.*, vol. 60, no. 4, pp. 351–354, 1941.
- [13] P. W. Bridgman, "Polymorphism, principally of the elements, up to 50,000 kg/cm²," *Phys. Rev.*, vol. 48, no. 11, pp. 893–906, 1935.
- [14] G. J. Piermarini, "Alvin van valkenburg and the diamond anvil cell," *High Press. Res.*, vol. 11, no. 5, pp. 279–284, 1993.
- [15] W. A. Bassett, "Diamond anvil cell, 50th birthday," *High Press. Res.*, vol. 29, no. 2, pp. 163–186, 2009.
- [16] D. J. Dunstan, "Theory of the gasket in diamond anvil high-pressure cells," *Rev. Sci.*

- Instrum.*, vol. 60, no. 12, pp. 3789–3795, 1989.
- [17] S. Klotz, J. C. Chervin, P. Munsch, and G. Le Marchand, “Hydrostatic limits of 11 pressure transmitting media,” *J. Phys. D. Appl. Phys.*, vol. 42, no. 7, 2009.
- [18] S. V. Rashchenko, A. Kurnosov, L. Dubrovinsky, and K. D. Litasov, “Revised calibration of the Sm:SrB₄O₇ pressure sensor using the Sm-doped yttrium-aluminum garnet primary pressure scale,” *J. Appl. Phys.*, vol. 117, no. 14, 2015.
- [19] Q. Jing *et al.*, “An experimental study on SrB₄O₇:Sm²⁺ as a pressure sensor,” *J. Appl. Phys.*, vol. 113, no. 2, 2013.
- [20] F. Datchi, R. LeToullec, and P. Loubeyre, “Improved calibration of the SrB₄O₇: Sm²⁺ optical pressure gauge: Advantages at very high pressures and high temperatures,” *J. Appl. Phys.*, 1997.
- [21] D. M. Trots *et al.*, “The Sm:YAG primary fluorescence pressure scale,” *J. Geophys. Res. Solid Earth*, vol. 118, no. 11, pp. 5805–5813, 2013.
- [22] S. V. Raju *et al.*, “Determination of the variation of the fluorescence line positions of ruby, strontium tetraborate, alexandrite, and samarium-doped yttrium aluminum garnet with pressure and temperature,” *J. Appl. Phys.*, vol. 110, no. 2, 2011.
- [23] A. F. Goncharov, J. M. Zaug, J. C. Crowhurst, and E. Gregoryanz, “Optical calibration of pressure sensors for high pressures and temperatures,” *J. Appl. Phys.*, vol. 97, no. 9, 2005.
- [24] A. Dewaele, M. Torrent, P. Loubeyre, and M. Mezouar, “Compression curves of transition metals in the Mbar range: Experiments and projector augmented-wave calculations,” *Phys. Rev. B - Condens. Matter Mater. Phys.*, vol. 78, no. 10, pp. 1–13, 2008.
- [25] H. K. Mao, P. M. Bell, J. W. Shaner, and D. J. Steinberg, “Specific volume measurements of Cu, Mo, Pd, and Ag and calibration of the ruby R1 fluorescence pressure gauge from 0.06 to 1 Mbar,” *J. Appl. Phys.*, vol. 49, no. 6, pp. 3276–3283, 1978.
- [26] L. Liu, Y. Bi, and J. A. Xu, “Ruby fluorescence pressure scale: Revisited,” *Chinese Phys. B*, vol. 22, no. 5, 2013.
- [27] F. Datchi, A. Dewaele, P. Loubeyre, R. Letoulllec, Y. Le Godec, and B. Canny, “Optical pressure sensors for high-pressure-high-temperature studies in a diamond anvil cell,” *High Press. Res.*, vol. 27, no. 4, pp. 447–463, 2007.
- [28] Z. Jenei, H. Cynn, K. Visbeck, and W. J. Evans, “High-temperature experiments using a resistively heated high-pressure membrane diamond anvil cell,” *Rev. Sci. Instrum.*, vol. 84, no. 9, 2013.
- [29] R. Boehler, M. F. Nicol, C. S. Zha, and M. L. Johnson, “Resistance Heating of Fe and W in Diamond-Anvil Cells,” *Phys. 139 & 140B*, pp. 916–918, 1986.

- [30] D. Schiferl, "Temperature compensated high-temperature/high-pressure Merrill-Bassett diamond anvil cell," *Rev. Sci. Instrum.*, vol. 58, no. 7, pp. 1316–1317, 1987.
- [31] W. A. Bassett, A. H. Shen, M. Bucknum, and I. M. Chou, "A new diamond anvil cell for hydrothermal studies to 2.5 GPa and from -190 to 1200 °C," *Rev. Sci. Instrum.*, vol. 64, no. 8, pp. 2340–2345, 1993.
- [32] Y. Fei and H. K. Mao, "In situ determination of the NiAs phase of FeO at high pressure and temperature," *Science (80-.)*, 1994.
- [33] L. S. Dubrovinsky, S. K. Saxena, and P. Lazor, "High-pressure and high-temperature in situ X-ray diffraction study of iron and corundum to 68 GPa using an internally heated diamond anvil cell," *Phys. Chem. Miner.*, vol. 25, no. 6, pp. 434–441, 1998.
- [34] N. M. Balzaretti, E. J. Gonzalez, G. J. Piermarini, and T. P. Russell, "Resistance heating of the gasket in a gem-anvil high pressure cell," *Rev. Sci. Instrum.*, vol. 70, no. 11, pp. 4316–4323, 1999.
- [35] C.-S. Zha and W. A. Bassett, "Internal resistive heating in diamond anvil cell for in situ x-ray diffraction and Raman scattering," *Rev. Sci. Instrum.*, vol. 74, no. 3, pp. 1255–1262, 2003.
- [36] N. Dubrovinskaia and L. Dubrovinsky, "Whole-cell heater for the diamond anvil cell," *Rev. Sci. Instrum.*, vol. 74, no. 7, pp. 3433–3437, 2003.
- [37] S. Pasternak *et al.*, "A diamond anvil cell with resistive heating for high pressure and high temperature x-ray diffraction and absorption studies," *Rev. Sci. Instrum.*, vol. 79, no. 8, 2008.
- [38] S. T. Weir, D. D. Jackson, S. Falabella, G. Samudrala, and Y. K. Vohra, "An electrical microheater technique for high-pressure and high-temperature diamond anvil cell experiments," *Rev. Sci. Instrum.*, vol. 80, no. 1, 2009.
- [39] S. T. Weir, M. J. Lipp, S. Falabella, G. Samudrala, and Y. K. Vohra, "High pressure melting curve of tin measured using an internal resistive heating technique to 45 GPa," *J. Appl. Phys.*, vol. 111, no. 12, 2012.
- [40] Z. Du, L. Miyagi, G. Amulele, and K. K. M. Lee, "Efficient graphite ring heater suitable for diamond-anvil cells to 1300 K," *Rev. Sci. Instrum.*, vol. 84, no. 2, 2013.
- [41] K. Yamamoto, S. Endo, A. Yamagishi, H. Mikami, H. Hori, and M. Date, "A ceramic-type diamond anvil cell for optical measurements at high pressure in pulsed high magnetic fields," *Rev. Sci. Instrum.*, vol. 62, no. 12, pp. 2988–2990, 1991.
- [42] D. A. Long, *Raman Spectroscopy*. New York: McGraw-Hill, 1977.
- [43] S. V. Goryainov, E. N. Kolesnik, and E. V. Boldyreva, "A reversible pressure-induced phase transition in β -glycine at 0.76 GPa," *Phys. B Condens. Matter*, vol. 357, no. 3–4, pp. 340–347, 2005.

- [44] C. Murli, S. M. Sharma, S. Karmakar, and S. K. Sikka, "α-Glycine under high pressures: A Raman scattering study," *Phys. B Condens. Matter*, vol. 339, no. 1, pp. 23–30, 2003.
- [45] S. A. Moggach, W. G. Marshall, D. M. Rogers, and S. Parsons, "How focussing on hydrogen bonding interactions in amino acids can miss the bigger picture: A high-pressure neutron powder diffraction study of ε-glycine," *CrystEngComm*, vol. 17, no. 28, pp. 5315–5328, 2015.
- [46] S. V. Goryainov, E. V. Boldyreva, and E. N. Kolesnik, "Raman observation of a new (ζ) polymorph of glycine?," *Chem. Phys. Lett.*, vol. 419, no. 4–6, pp. 496–500, 2006.
- [47] E. V. Boldyreva, V. A. Drebushchak, T. N. Drebushchak, I. E. Paukov, Y. A. Kovalevskaya, and E. S. Shutova, "Polymorphism of glycine, Part I," *J. Therm. Anal. Calorim.*, vol. 73, no. 2, pp. 409–418, 2003.
- [48] E. V. Boldyreva, V. A. Drebushchak, T. N. Drebushchak, I. E. Paukov, Y. A. Kovalevskaya, and E. S. Shutova, "Polymorphism of glycine, Part II," *J. Therm. Anal. Calorim.*, vol. 73, pp. 419–428, 2003.
- [49] V. A. Drebushchak, E. V. Boldyreva, T. N. Drebushchak, and E. S. Shutova, "Synthesis and calorimetric investigation of unstable β-glycine," *J. Cryst. Growth*, vol. 241, no. 1–2, pp. 266–268, 2002.
- [50] E. L. Crowell, Z. A. Dreger, and Y. M. Gupta, "High-pressure polymorphism of acetylsalicylic acid (aspirin): Raman spectroscopy," *J. Mol. Struct.*, vol. 1082, pp. 29–37, 2014.
- [51] E. J. Chan, T. R. Welberry, A. P. Heerdegen, and D. J. Goossens, "Diffuse scattering study of aspirin forms (I) and (II)," *Acta Crystallogr. Sect. B Struct. Sci.*, vol. 66, no. 6, pp. 696–707, 2010.
- [52] A. D. Bond, R. Boese, and G. R. Desiraju, "On the polymorphism of aspirin," *Angew. Chemie - Int. Ed.*, vol. 46, no. 4, pp. 615–617, 2007.
- [53] N. Zaitseva *et al.*, "Application of solution techniques for rapid growth of organic crystals," *J. Cryst. Growth*, vol. 314, no. 1, pp. 163–170, 2011.
- [54] R. Letoullec, J. P. Pinceaux, and P. Loubeyre, "The Membrane Diamond Anvil Cell: A New Device For Generating Continuous Pressure And Temperature Variations," *High Press. Res.*, vol. 1, no. 1, pp. 77–90, 1988.
- [55] B. Z. Chowdhry, T. J. Dines, S. Jabeen, and R. Withnall, "Vibrational spectra of α-amino acids in the zwitterionic state in aqueous solution and the solid state: DFT calculations and the influence of hydrogen bonding," *J. Phys. Chem. A*, vol. 112, no. 41, pp. 10333–10347, 2008.
- [56] P. Le Couteur and J. Burreson, *Napoleon's buttons: 17 molecules that changed history*. Penguin, 2004.

- [57] A. Eckert, "Organ pipes and tin pest," *Mater. Corros.*, vol. 59, no. 3, pp. 254–260, 2008.
- [58] R. W. Smith, "The Semi-Conductor \rightleftharpoons Metal Transition in Tin," *J. Less-Common Met.*, vol. 114, pp. 69–80, Jan. 1986.
- [59] A. Salamat *et al.*, "High-pressure structural transformations of Sn up to 138 GPa: Angle-dispersive synchrotron x-ray diffraction study," *Phys. Rev. B*, vol. 88, no. 10, p. 104104, 2013.
- [60] J. D. BARNETT, R. B. BENNION, and H. T. HALL, "X-ray Diffraction Studies on Tin at High Pressure and High Temperature," *Science (80-.)*, vol. 141, no. 3585, pp. 1041–1043, 1963.
- [61] J. D. Dudley and H. T. Hall, "Experimental fusion curves of indium and tin to 105 000 atmospheres," *Phys. Rev.*, vol. 118, no. 5, pp. 1211–1216, 1960.
- [62] P. A. Folkes, P. Taylor, C. Rong, B. Nichols, H. Hier, and M. Farrell, "Raman Scattering from Tin," 2015.
- [63] E. Kroumova *et al.*, "Bilbao Crystallographic Server: Useful databases and tools for phase-transition studies," *Phase Transitions*, vol. 76, no. 1–2, pp. 155–170, 2003.
- [64] H. Giefers *et al.*, "Phonon density of states of metallic Sn at high pressure," *Phys. Rev. Lett.*, vol. 98, no. 24, pp. 1–4, 2007.
- [65] M. M. A.-E. A. Barla, R. Ruffer, A. I. Chumakov, J. Metge, J. Plessel, "Direct determination of the phonon density of states in B-Sn," *Phys. Rev. B*, vol. 61, no. 22, pp. 881–884, 2000.
- [66] J. K. Hinton *et al.*, "Effects of pressure on the structure and lattice dynamics of α -glycine: a combined experimental and theoretical study," *CrystEngComm*, 2019.
- [67] J. S. C. Kearney *et al.*, "Pressure-Tuneable Visible-Range Band Gap in the Ionic Spinel Tin Nitride," *Angew. Chemie - Int. Ed.*, vol. 57, no. 36, pp. 11623–11628, 2018.

Jasmine Hinton

Curriculum Vitae

jasmine.k.hinton@gmail.com

Education

| | | | |
|---------------------------------|-------|---------|--------------------|
| University of Nevada, Las Vegas | M.Sc. | Physics | 08/2016 to Present |
| University of Utah | B.Sc. | Physics | 06/2012 to 05/2016 |
| Utah Valley University | A.Sc. | General | Completed 04/2012 |

Publications

- “Effects of Pressure on the structure and lattice dynamics of α -glycine: A combined experimental and theoretical study” **J.K. Hinton**, S. Clarke, B.A. Steele, F.W. Kuo, E. Greenberg, V.B. Prakapenka, M. Kunz, M.P. Kroonblawd, E. Stavrou (*CyrstEngComm*) 2019
- “Pressure-Tunable Visible-Range Band Gap in the Ionic Spinel Tin Nitride.” J. S. C. Kearney, M. Grauzinyte, D. Smith, D. Sneed, C. Childs, **J. Hinton**, C. Park, J. S. Smith, E. Kim, S. D. S. Fitch, A. L. Hector, C. J. Pickard, J. A. Flores-Livas,* and A. Salamat (*Angewandte Chemie* p11623-11628, 2018)
- “Deuterium Isotope Effects in Polymerization of Benzene Under Pressure.” W. Cai, M. Dunuwille, J. He, T. Taylor, **J.K. Hinton**, M. MacLean, J. Molaison, A. dos Santos, S. Sinogeikin, S. Deemyad. (*Journal of Physical Chemistry Letters* p1856-1864, 2017)
- “Superconducting Phase Diagram of 6 Li: Anomalous Isotope Effects in Superconducting Dense Lithium.” A.M. Schaeffer, S.R. Temple, **J.K. Bishop**, S. Deemyad: (*Proceedings of the National Academy of Sciences* p60-64, 2015; arXiv:1406.4565, 12-22-2014)

Research Interests

I’m interested in exploring exotic new and metastable phases of systems with rich polymorphism using high pressure and high temperature. I also hope to further develop and improve instrumentation to aid my research goals, including advancing diamond anvil cell and resistive heating techniques.

Honors and Awards

- Excellent Poster Award from Poster symposium at Beijing AIRAPT 2017
- Student Grant to attend AIRAPT 2017
- UROP travel award and Department travel award to travel to the Advance Photon Source at Argonne National Lab (2015)
- REU Summer Program Funding Award (2015)
- Research Experience at the Advanced Light Source at Berkeley National Lab (2015)
- Martin Hiatt Outstanding Undergraduate Research Award (2015)
- Parmley Scholarship (2015)
- Best Undergraduate Oral Presentation at APS Four Corners (2014)
- Accepted into the High Pressure Gordon Research Conference (2014)
- UROP Assistantship for two semesters (2013-2014)
- New Century Scholarship for four semesters (2012-2014)
- ACCESS Program for Women in Science (Summer 2012-Spring 2013)
- Honors at Entrance Scholarship (2012-2016)

Relevant Work Experience

| | | |
|---------------------|----------------------|--------------|
| LLNL Internship | (Student Researcher) | May—Aug 2018 |
| Ripple Neuroscience | (Hardware Tester) | Feb—Aug 2016 |

Highlighted Skills

- Preparing Diamond Anvil Cell
- *In situ* resistive heating
- Synthesis of Organic Crystals
- Excellent at scientific writing/communication
- Raman and Fluorescence Spectroscopy
- Data Analysis in Origin, GSASII & DIOPTAS
- Crafting in machine shop

Teaching

- PHYS 180L – (F16, S17, F17, S18) Introductory mechanics labs for scientists and engineers
- PHYS 151L – (F16, S17, F17) Introductory mechanics labs for non-majors
- PHYS 181L – (F18) Applied electricity and magnetism in beginner circuitry
- PHYS 152L – (S18, F18) Introductory circuits and optics (a combo of 181 & 182)
- PHYS 182L – (S19, S19) Wave mechanics, fluids, specific heat, and optics

Outreach/Workshops

| | |
|--|--|
| Rebel STEM Academy | (GA/lab activity guide April 2017) |
| Quadrennial Physics Congress (PhysCon) | (exhibitor for UNLV Nov 2016) |
| Extreme Crystals Weekend | (participant in Mar 2016 and volunteer in Oct 2016 & 2017) |

Presentations

- **J.K. Hinton**, E. Stavrou: “Structural Study of α -glycine under Extreme Conditions,” (Poster LLNL 2018)
- **D. Smith, J.K. Hinton**, A. Salamat: “Extreme Conditions Research at the Salamat Lab” (Joint poster, SSAA symposium 2018)
- **J.K. Hinton**, Q. Zhu, A. Salamat: “Melt Crystallization; a novel route to metastable states in simple organic systems” (Poster, AIRAPT Beijing 2017); (Poster, SSAA symposium 2017); (Poster, GRC 2018)
- A.M. Schaeffer, **J.K. Bishop**, S.R. Temple, S. Deemyad: “Investigating the Possible Temperature Dependence of 6Li Phase Diagram Under Pressure” (Talk, REU Symposium 2015)
- **J.K. Bishop**, A.M. Schaeffer, F. Doval, S. Deemyad: “Re-emergent Superconductivity of KFeSe Under Pressure”(Talk, UROP symposium Spring 2015); (Talk, APS Four Corners 2014)
- A.M. Schaeffer, S.R. Temple, **J.K. Bishop**, S. Deemyad: “Superconducting Phase Diagram of 6 Li: Anomalous Isotope Effects in Superconducting Dense Lithium ”Talks: (REU Symposium 2014); (UROP Symposium 2014); (UCUR at BYU 2014)
- **J.K. Bishop**, A.M. Schaeffer, F. Doval, S. Deemyad: “Pressure Analysis of Twin Chamber Gaskets in Diamond Anvil Cells” (Poster, Gordon Research Conference 2014)
- **J.K. Bishop**, A.M. Schaeffer, S.R. Temple, J.Jue, Z., Xu, S. Deemyad: “Physics at Extreme Conditions” (Poster, APS Conference for Undergraduate Women in Physics, University of Utah 2013); (Talk, UROP symposium, University of Utah 2013); (Poster, ACCESS Poster Session, University of Utah 2013)